T H E U N I V E R S I T Y O F M I C H I G A N

COLLEGE OF LITERATURE, SCIENCE, AND THE ARTS
Department of Physics

Technical Report

THE NEUTRAL DECAY MODE OF THE LAMBDA HYPERON AS OBSERVED IN A XENON BUBBLE CHAMBER

Howard C. Bryant

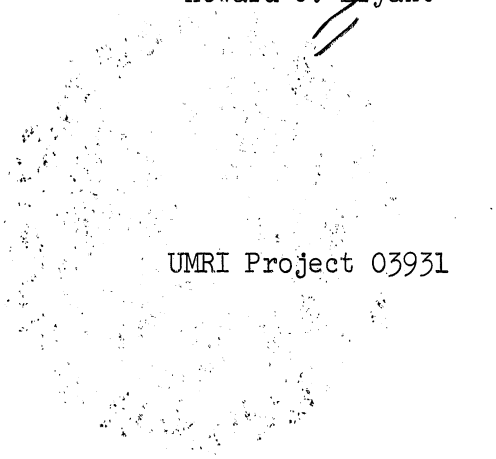

UMRI Project 03931

under contract with:

U. S. ATOMIC ENERGY COMMISSION
CONTRACT NO. AT(11-1)-363
CHICAGO OPERATIONS OFFICE
ARGONNE, ILLINOIS

administered by:

THE UNIVERSITY OF MICHIGAN RESEARCH INSTITUTE ANN ARBOR

August 1960

This report has also been submitted as a dissertation in partial fulfillment of the requirements for the degree of Doctor of Philosophy in The University of Michigan, 1960

TABLE OF CONTENTS

LIST OF TABLES

LIST OF FIGURES

LIST OF FIGURES (concluded)

ABSTRACT

The decay of the lambda hyperon into a neutral pion and a neutron has long been suspected and indeed has been indirectly observed electronically and in a bubble chamber. For about half of such neutral decays that occur in a xenon bubble chamber both gamma rays from the decay of the neutral pion convert into electron-positron pairs. This high conversion probability makes possible a rather clear-cut identification of such events.

In an exposure of The University of Michigan xenon bubble chamber to a beam of negative pions of about one billion electron volts kinetic energy, thirty-two events of the above described type were found in association with charged decays of the neutral theta meson in pictures of high visibility. On the basis of these events and ninety-six events of the charged-pionic decay mode of the lambda, with the same conditions as were applied to the neutral events, the rate of neutral decay to all pionic decays for the lambda hyperon is 0.35 ± 0.05. The ratio of the neutral mode asymmetry parameter to the charged mode asymmetry parameter is found to be 1.16 ± 0.97, and the mass (in terms of its energy equivalent) of the neutral pion from the lambda decay is found to be 126 ± 7 million electron volts.

DEFINITIONS OF COMMON OR IMPORTANT SYMBOLS

M_Λ, M_{π°, M_n	Mass of the Λ, π°, neutron in Mev.
P_Λ	Momentum of the Λ in Mev/c.
L_Λ	Distance of decay of Λ from point of production in cm.
V	V-shaped bubble-track configurations which could be due to the decay of a neutral particle into two charged particles.
δ	"Coplanarity angle," the angle between the plane of the V and the line joining its apex to the presumed origin.
θ	The angle between the two legs of a V.
θ_1, θ_2	The angle between leg 1, 2 of a V and the line joining the apex and the presumed origin. ("π" or "p" can be substituted for "1" or "2" to indicate knowledge of type of particle involved.)
θ_1^*, θ_2^*	Angle in the CM made by leg 1, 2 of a V and the line of flight of the particle which decayed into the V.
R_1, R_2	The range of leg 1, 2 in the xenon chamber.
Δ	The distance of closest approach between two gamma rays as predicted from the electron pairs which they produce.
Δ_k	The distance one must move the 2nd point of the direction measurement of the k^{th} electron pair in order that the gamma ray k appears to come from an arbitrary point of origin.
ω	"Production angle," the angle the line of flight of a particle makes with the direction of the beam track from which it was produced.
ABC, ABD	Used to indicate the category of events which satisfy criteria A, B and C, D given in chapter 4, or the <u>number</u> in the category ABC, ABD.
σ_k	The correction factor in the k^{th} bias enumerated in chapter 4 used in computing the neutral branching ratio.

DEFINITIONS OF COMMON OR IMPORTANT SYMBOLS (concluded)

R	The ratio of the rate of $\Lambda \longrightarrow \pi^{\circ} + n$ to the rate of $\Lambda \longrightarrow \pi^{-} + p$.
B_{Λ}	The neutral branching ratio defined as R/1 + R. The angle between the directions of two associated gamma rays as determined by their electron pairs.
LAB	The laboratory coordinate system.
RMS	Root mean square.
CM	The center-of-mass coordinate system.

I. INTRODUCTION

Since the first convincing proof for the existence of the Λ hyperon was presented in 1951 (1), much work has been done to determine its physical properties, the latest values for which are given in Table I. Although for several years the only observations of the particle were through the decay mode, $\Lambda \longrightarrow \pi^- + p$, it was expected that the mode, $\Lambda \longrightarrow \pi^\circ + n$, should also occur.

The first attempts to observe this mode were done with counters using an "extended source" technique (1). This method involves measuring the apparent size of a gamma source consisting of a target in a beam of protons. Since the lifetime of the π° meson is less than 10^{-15} seconds, the π°'s produced directly will not increase the apparent size of the source. However, if relatively long-lived particles, say of lifetimes of the order of 10^{-10} seconds, which decay into gammas either directly or through a π° intermediary, are produced, the apparent size of the source as observed with counter-telescopes will appear to increase to a size depending on the velocity distributions and lifetimes of the parent particles. Moreover, as one lowers the energy of the proton beam below the thresholds for production of the parent particles, one should observe a disappearance of the extended source. This method indeed yielded strong, but indirect, evidence for the existence of the neutral mode of the Λ.

Next Eisler et al (2) in a propane bubble chamber looked for electron pairs in association with K_1° mesons from the reaction

$$\pi^- + p \longrightarrow \Lambda + K^\circ.$$

They found 5 such gamma-produced pairs, which, making use of the production kinematics and the measured momentum of the K_1°, they were able to show were consistent with coming from the decay of the π° from $\Lambda \longrightarrow \pi^\circ + n$, but not

consistent with a scheme such as $\Lambda \longrightarrow$ single gamma + neutron.

In 1955 Donald Glaser pointed out the usefulness of a heavy-liquid bubble chamber for the study of particle decay modes involving gamma rays (3), and in 1956 the operation of the first liquid xenon chamber was reported by the Michigan bubble chamber group (4). Shortly after, work was begun on a 21-liter chamber which was completed in the Spring of 1958 and taken to the Bevatron at Berkeley. During the summer of 1958 an exposure was made to π^- mesons of about 1.1 Bev kinetic energy and about 160,000 pictures were taken (5). The study of the neutral pionic decay mode of the Λ as observed in these pictures is the subject of this thesis.

Table 1. The Physical Properties of the Λ.

Mass = 1115.38 ± 0.13 Mev (6)

Spin = 1/2 (7)

Mean Life = $(2.505 \pm .086) \times 10^{-10}$ seconds (8)

Decay modes:

$\Lambda \rightarrow \pi^- + \text{proton}$

$\Lambda \rightarrow \pi^\circ + \text{neutron}$

$\Lambda \rightarrow \text{nucleon} + \text{lepton} + \text{neutrino}$ (9)

Pionic charged mode branching ratio:

$$\frac{w(\Lambda \rightarrow \pi^- + p)}{w(\Lambda \rightarrow \text{all modes})} = .627 \pm .031 \quad (10)$$

Asymmetry parameter of charged mode, absolute value:

$|\alpha_-| > 0.73 \pm 0.14$ (11)

Ratio of asymmetry parameters of two pionic modes:

$$\frac{\alpha_0}{\alpha_-} = +1.10 \pm .27 \quad (12)$$

<u>Properties determined in this thesis:</u>

Neutral pionic branching ratio:

$$\frac{w(\Lambda \rightarrow \pi^\circ + n)}{w(\Lambda \rightarrow \pi^\circ + n) + w(\Lambda \quad \pi^- + p)} = .35 \pm .05 \quad \text{page } 47$$

$\alpha_- \bar{P}$ (charged mode) = $.32 \pm .11$ page 50

$\alpha_0 \bar{P}$ (neutral mode) = $.37 \pm .28$ page 51

$$\frac{\alpha_{0\,\text{neutral}}}{\alpha_{-\,\text{charged}}} = 1.16 \pm .97 \quad \text{page } 51$$

Mean Life (from charged mode) = $\left(2.77 \, {}^{+.48}_{-.34} \right) \times 10^{-10}$ seconds page 52

Mass of the π° from the Λ decay = 126 ± 6 Mev page 58

II. EXPERIMENTAL ARRANGEMENT

The Bubble Chamber Exposure

A schematic diagram of the xenon bubble chamber as it was during the summer of 1958 when this experiment was done can be seen in Fig. 1. Table 2 summarizes the important properties of the chamber.

In late June, 1958, the xenon bubble chamber was placed in a concrete block house on the Bevatron floor at Berkeley. Using a bending magnet and a quadrupole focussing magnet a π^- beam passing through a H_2 target being used by Cool et al (13) was made to pass through the center of the bubble chamber. Since the Cool experiment was a counter experiment which required the beam to be spread over a time interval of about one hundred milliseconds in order to avoid "pileup", and since for uniform bubble size in a bubble chamber the beam should be less than a millisecond in duration, it was convenient to use the "Rapid Beam Ejector" RBE, modelled after a design by Dr. David Rahm of Brookhaven, by means of which about five percent of the total π^- beam could be delayed and formed into a spike about fifteen milliseconds after the main beam had passed through the apparatus. The timing of the expansion of the bubble chamber was adjusted so that the chamber was sensitive only to the particles occurring in the spike. A schematic diagram of the electronics associated with the chamber and a profile of the pressure pulse during an expansion of the chamber can be seen in Fig. 2.

The beam intensity at the chamber was monitored by means of a plastic scintillator placed in front of the beam window of the bubble chamber and gated with a two millisecond gate centered on the RBE pulse, and the counts displayed on a scaler. The signal from the counter was also displayed in the control room of the Bevatron where by use of the "beam shaper" and much patience the operating crew was able to clean up the stray beam particles occurring in the sensitive region of the pressure pulse, thus improving greatly the quality of the pictures

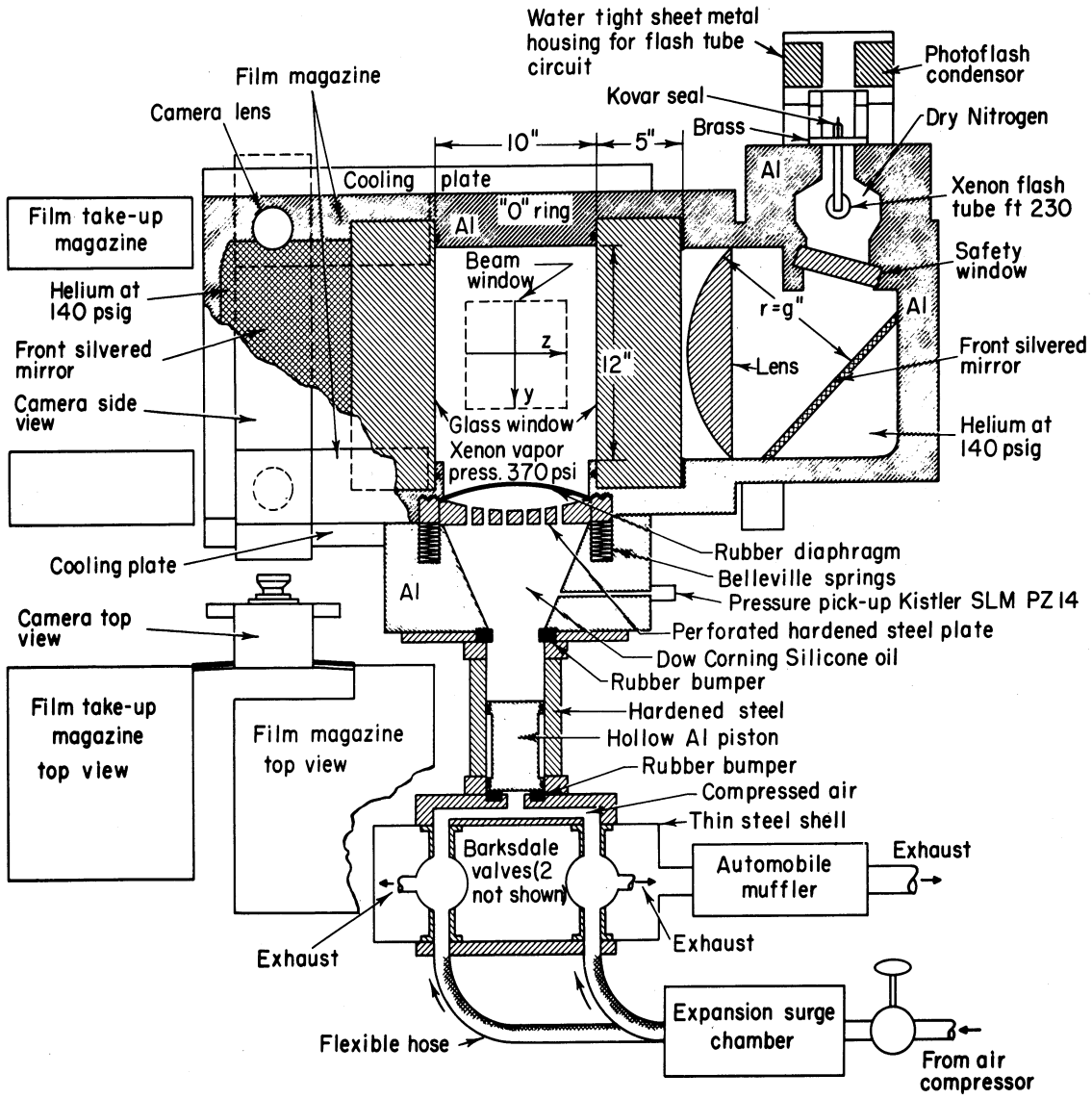

Fig. 1. Michigan Xenon Bubble Chamber, Summer 1958.

Table 2. Bubble Chamber Properties

Chamber Dimensions

Active volume: 10" deep; 12" diameter; 21 liters

Glass windows: 5" thick; 15" diameter

Distance between camera lenses: 14 3/8"

Distance from lens of camera to center of the chamber: 26"

Cylinder diameter: 3.9940 $\pm$ .0005"

Piston travel distance: 3 31/32"

Displacement: 0.82 liters

Expansion System

Diaphragm: Raybestus-Manhattan 2-ply nylon in buna "n" 683, 1/8" thick

Supporting fluid: Dow-Corning "200" Silicone Oil

Barksdale valves: 4 of them, inside diameter 3/4"

Compressor pressure: 420-430 p.s.i.g.

Free volume: 2.7-3.0%

Pressure pickups: SLM PZ-14, Kistler Instrument Co. (Quartz-piezoelectric)

Cooling System

Coolant: 50-50 mixture of ethylene glycol and water

Refrigerator: 2-ton G.E. designed by Mr. Hugh J. Scullen of Detroit

Optical System

Light source: General Electric FT 230 (operating voltage about 1500 volts d.c. and capacitance of about 45 microfarads)

Duration of light pulse: 100 microseconds

Light delay after beam: about 1.5 milliseconds

Chamber illumination optics: dark field

Collimation lens: 18" focal length; 12" diameter

Mirrors: front-silvered

Camera: F stop f/45

Film: Kodak Linagraph Panchromatic 70 mm. (blue-gray acetate with resolving power of 70 lines per mm.)

Xenon Parameters at Operating Conditions

$T = (-21.5 \pm 0.1)°C$

Density = 2.17 grams/cm.^{3}

Vapor pressure = 370 p.s.i.g.

Radiation length = 3.9 cm.

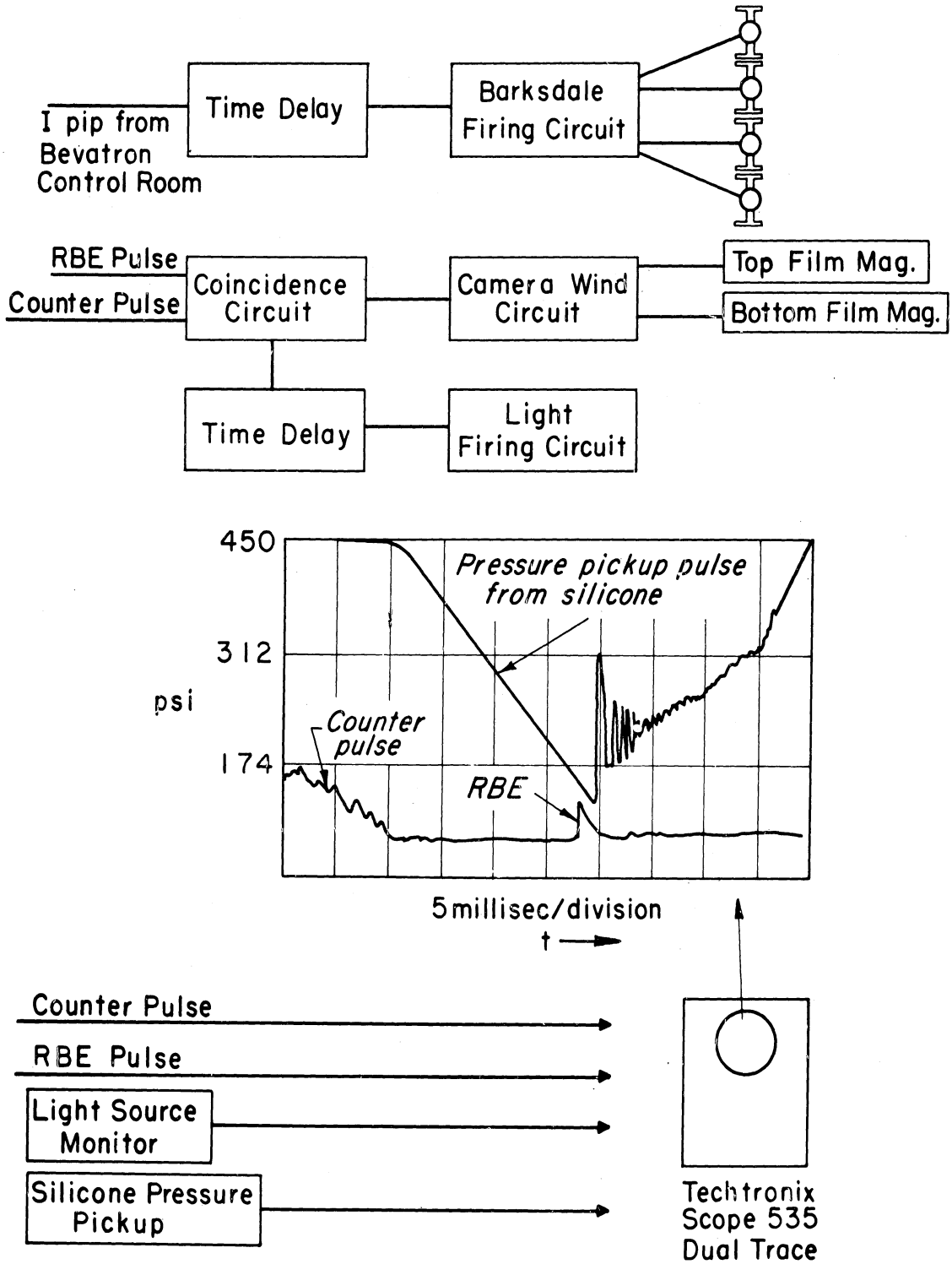

Schematic of Bubble Chamber Electronics
Summer 1958

Fig. 2. Schematic of Bubble Chamber Electronics, Summer 1958.

from this run. By monitoring the beam in this way the number of unusable pictures due to too many tracks (sixteen or more) was kept at a minimum. The light was fired by a pulse delayed about 1.5 milliseconds after the RBE. The light was monitored with a phototube in order that its intensity could be kept constant. The duration of the light flash was about 100 μseconds. We found that the number of tracks could also be monitored visually by looking through a peephole that had been built into the chamber in order to observe the xenon level.

The temperature of the aluminum body of the bubble chamber was regulated to $-(21.5 \pm 0.1)$ degrees centigrade and since the operation and timing were rather precise one expects that there were no appreciable fluctuations in the density of the xenon from picture to picture.

As the experiment progressed it was found that the xenon gradually became cloudy due to opaque residue from the rubber diaphragm. The xenon was removed and replaced twice during the run; this process involves distillation which leaves much of the residue in the storage tanks.

The kinetic energy of the beam was set by the Cool experiment and was about 1.0 Bev for the first 60,000 frames and 1.1 Bev for the rest until 160,000, except for frames between the numbers 104,037 and 106,606 for which the beam energy dropped to 0.8 Bev for a background check for Cool. During the run about 1000 frames of π^+ mesons were also taken; these will not be discussed in this paper. We did not independently measure the momentum of the beam during the experiment. The purity of the beam was not measured.

Data Handling

After the film was developed by the photographic lab at the Lawrence Radiation Laboratory it was cut up into 100 foot rolls of 400 frames each and sent to the High Energy Lab at the University of Michigan for scanning, measuring

and analysis.

The scanning of the pictures was done in a quonset hut located on East University in four specially constructed scanning booths. The scanning booths were constructed so that the two views of each frame could be projected completely independent of each other onto a white table top in front of the observer. The images were a little larger than life size. Because of this independent motion of the two views of the same exposure one could easily determine the parallax of a point in the chamber and thus roughly determine its position quite easily. We found that a good scanner could look through about 100 frames an hour. Sketches were made of all events that were of interest. A more detailed discussion of the scanning as it is related to this thesis will be given in the next chapter.

After the scanning of a roll was completed, the roll with its sketches of interesting events was returned to room 3071 Randall Laboratory where the events noted as being of interest were projected on one of the two "Green Screens" (precision measuring devices, so called because of the green coating on the projection glass), and if the event was deemed "real" by the measurer, the event was measured. The definition of "real" varied as the measuring progressed due to experience as noted in the next chapter. An event was real as far as this thesis is concerned if it did not clearly violate any of the criteria for scanners and measurers as given in the next chapter.

The Measuring Devices

The Green Screens were equipped with two sets of interchangeable lenses, one set giving a magnification of about 1.75 life size and the other set giving a magnification of about 4 times life size. The Green Screens enabled one to get a much better look at the events noted by the scanners, and events found to be not real were rejected at this stage.

The two Green Screens differed in particulars but their main features were the same. A coding system was set up so that each point of any particular event could be designated by a three-digit number. The stages were digitized so that their positions could be punched directly on IBM cards. In order to measure the spatial coordinates of a particular point in the chamber, one moved the stage of the Green Screen so that the image of the point in the view was centered on a fiducial crosshair on the screen; then one set the point's coded designation on a dial and pushed the read-out button, which automatically recorded both the coordinates of the stage and the point designation. Repetition of this procedure for the other stereo view of the point completed the measurement. In this manner an event could be measured in about 15 minutes (about 16 points). Checks were frequently made for encoder errors.

Computations

The method of handling the data cards evolved considerably during the course of analysis of these pictures, going from a rather cumbersome procedure using the IBM 650 to a very convenient one using the IBM 704 that was installed on the Michigan Campus in the Fall of 1959. The final IBM program, developed by Mr. Richard Hartung, computed first the spatial coordinates of the measured points in the bubble chamber and then all the geometrical properties of the array of points as called for by their code numbers.

The next step was the analysis of the measurements and the computed quantities. By means of range-energy curves and kinematics graphs the events were checked for consistency and identified and classified. Details of this process as related to the subject of this thesis will also be given in the next chapter.

Finally, if any questions remained about the classification of a particular

event, it was rescanned on a Green Screen, and perhaps remeasured.

At this point the data was available for various studies of which this thesis is but one of four.

III. DATA ANALYSIS

Data selection and assumptions:

The principal quantity to be determined about the neutral mode of the Λ in this thesis is the neutral pionic branching ratio defined as

$$B_\Lambda = \frac{W(\Lambda \rightarrow \pi^\circ + n)}{W(\Lambda \rightarrow \pi^\circ + n) + W(\Lambda \rightarrow \pi^- + p)}$$

where $W(x)$ is the rate of process x.

In determining this ratio we elect to use those Λ's from the reaction

$$\pi^- + \text{xenon nucleus} \rightarrow \Lambda + K^\circ + \text{residuals}$$

or

$$\pi^- + \text{xenon nucleus} \rightarrow \Sigma^\circ + K^\circ + \text{residuals}$$
$$(\Sigma^\circ \rightarrow \gamma + \Lambda)$$

for which the K° decays into two charged pions, i.e.

$$K_1^\circ \rightarrow \pi^+ + \pi^-$$

By restricting ourselves to the event-types described above we ignore a large fraction of the Λ's in the xenon chamber for which the charged K_1° mode does not occur. The reasons for making this restriction are

i. To avoid possible scanning bias due to the quite different appearances of the two Λ modes

$$\Lambda \rightarrow \pi^\circ + n \qquad \text{(two electron pairs)}$$

and

$$\Lambda \rightarrow \pi^- + p \qquad \text{(a "V")}$$

ii. To positively identify the Λ, especially the neutral mode.

We assume that electron pairs from converted gamma rays point to the position of the Λ decay, i.e. the "π°" occurring in the neutral mode of the Λ decay is the same one as observed in the reaction $\pi^- + p \rightarrow \pi^\circ + n$ (π^- absorption of hydrogen) and thus has a lifetime of about 10^{-16} seconds (14).

Scanning: Definitions

"V's" are defined as bubble-track configurations in which there is a discontinuity (known as the apex) in direction or bubble density.

"Legs of the V" are defined as the continuous segments of the V separated by the discontinuity.

"V origins" are defined to be beam-pion interactions such that the lines joining the interactions and the V-discontinuity pass between the two legs of the V in both stereo views.

"Associated electron pairs" are electron pairs that are consistent with having been produced by gamma rays which do not appear to come from beam or secondary interactions which are not V origins, but which occur in frames containing V's.

Instructions to scanners:

Scanners were instructed to look for V's with origins and to look for associated pairs. They were instructed to trace on a sheet of paper one view of any such event and to record a) the view (top or bottom camera), b) the frame number, c) the apparent bubble density of all tracks participating in the event (light, medium, or heavy), d) the apparent fate of each particle participating in the event (stops, interacts, or leaves the chamber), e) the number of beam tracks in the frame (lightly ionizing tracks less than 15° in direction from the "x-axis" defined below), f) the scanner's initials.

Bubble chamber coordinate system:

As seen in Fig. 1 the active volume of the chamber is a cylinder 10" long and 12" in diameter, bounded on the ends by two large cylindrical windows. The window through which the cameras "look" we call the "front" window and the window through which the illumination system shines we call the "back" window. Both front and back windows are scribed with grid marks (see Fig. 3) in a square array with spacing of 2 cm. and parallel to the stereo axis (the line joining the two camera lenses). The center grid mark of the front window we take as the origin of a right-handed Cartesian coordinate system with the x axis running parallel to the plane of the front window and perpendicular to the stereo axis and with the same sense and approximate direction of the π^- beam. The z axis is taken as normal to the front window with sense such that the z coordinate increases as one goes from front to back.

Measuring:

The measuring and analysis was done in two parts. The first part (I) consisted of the pictures up to frame number 86,000 and the second part (II) dealt with the pictures from 86,000 to 140,000. Part I was done first and the procedure was a little more involved and usually more tedious than that of part II for which we were able to take advantage of the experience gained in part I. The results of part I have already been reported (5B).

For part I each event with one or two V's with or without associated electron pairs was measured. For part II only those events having either two V's or one V and two or more associated electron pairs were measured although all events found by the scanners were carefully checked to insure that nothing had been missed. (Gamma pairs can easily be overlooked.)

A typical double V event (charged lambda and K_1° decays) and a rather good single K_1° with associated gamma pairs can be seen in Fig. 3 and Fig. 5. Fig. 4 shows the points that were measured on the neutral event shown in Fig. 5. The center grid mark (1) and the four corner grid marks (13, 14, 15, 16) were routinely measured to determine the absolute positions of the other points, to check on film shrinkage, and to check for rotation of the two views with respect to each other. Then all possible origins (2) for the V's were measured, and a second point (3) taken along the track to determine the beam direction. The apex point (4) was measured and points at appropriate points along each leg (5, 6, 7, 8), including the point at which the leg either stops or leaves the chamber. Each electron pair was measured at its apex (9, 11) and usually near the point where the two electron tracks appear to separate (10, 12). (One can show that the optimum point to measure for determination of the direction of the pair is near the separation point, although electron pairs at this energy, 20 to 200 Mev, suffer from rather violent statistical fluctuations.) The quantities pertaining to this paper computed by our final program are given in Table 3.

Examination of the computed spatial coordinates of several duplicate measurements of typical points in the chamber show that the RMS error in determining the location of points in the chamber is about .03 cm. For 22 duplicate measurements the average difference in the x and y coordinates was about .01 cm. and in the z, .02 cm.

The analysis of V's

The pertinent information for the identification and classification of V's is the coplanarity of the V with respect to the origin, δ, the opening angle, θ, the angles of the two legs with respect to the line of flight of

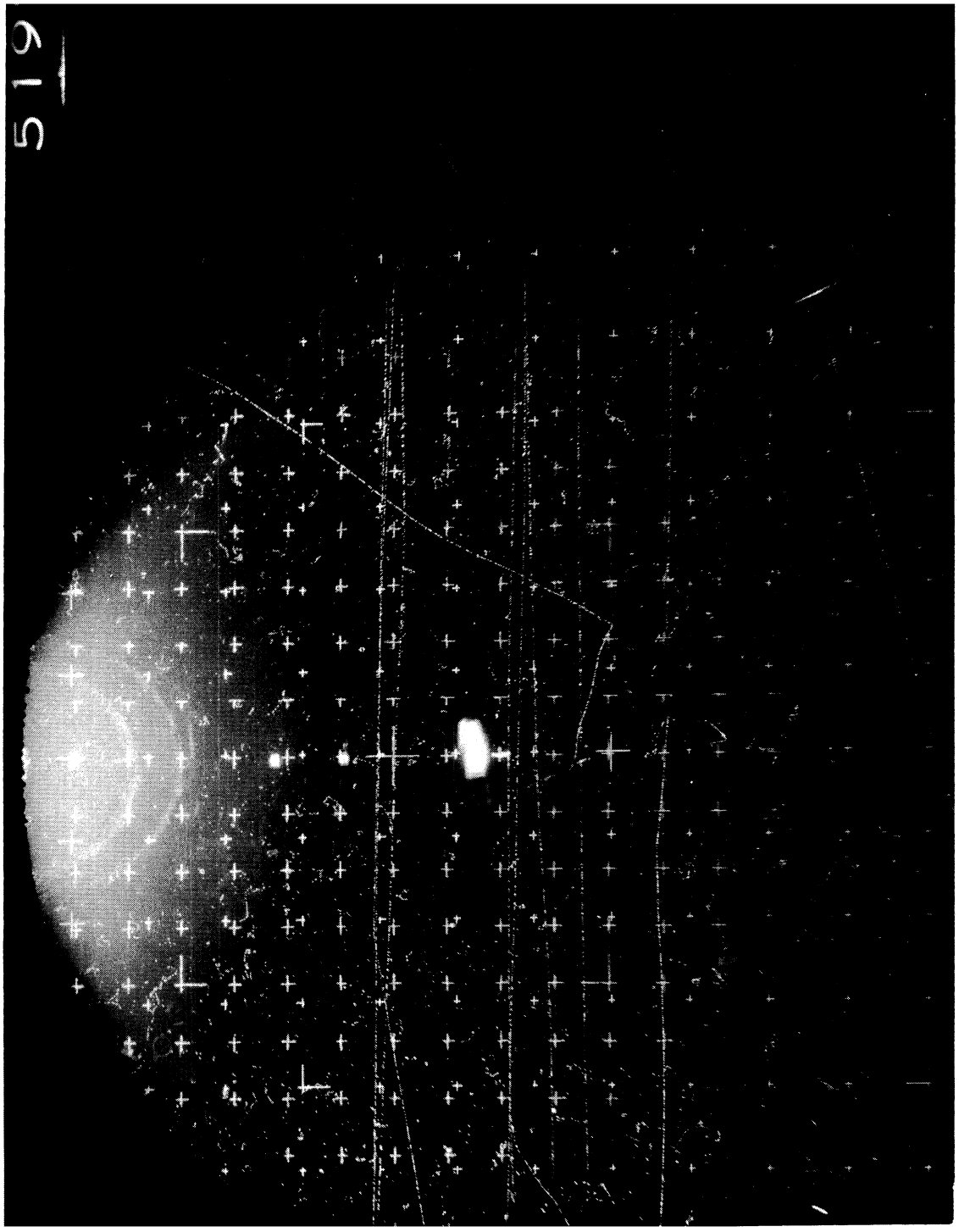

Fig. 3. Typical Double V Event.

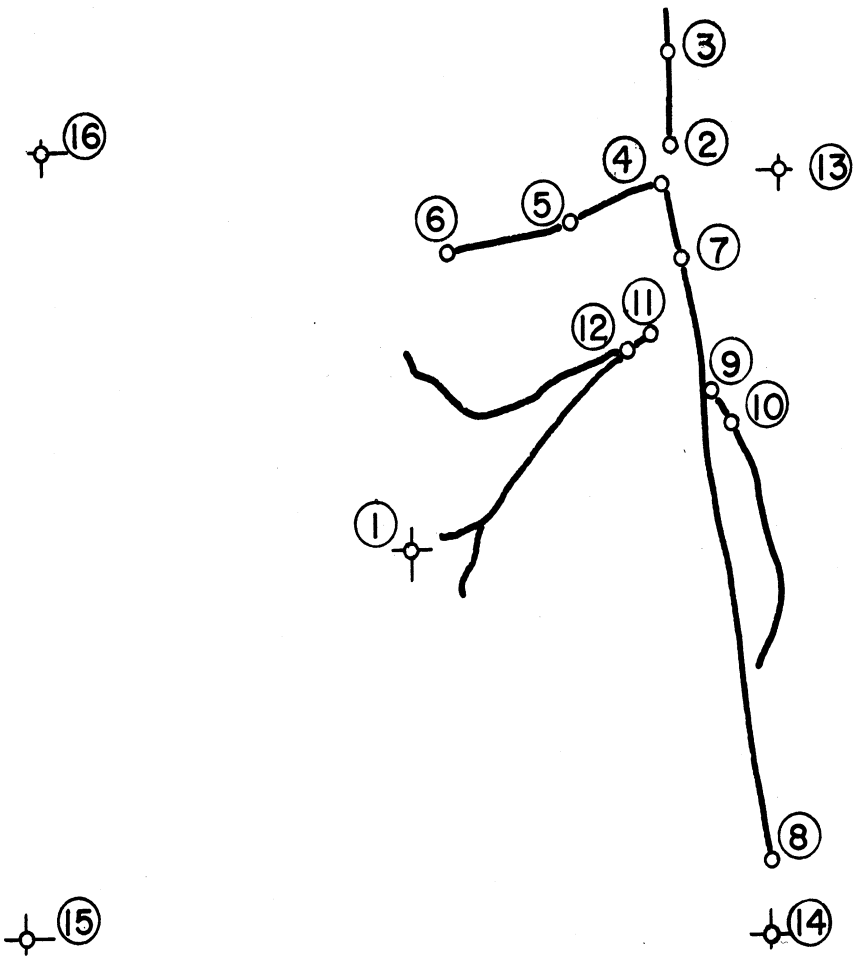

Fig. 4. Points Measured in Figure 5.

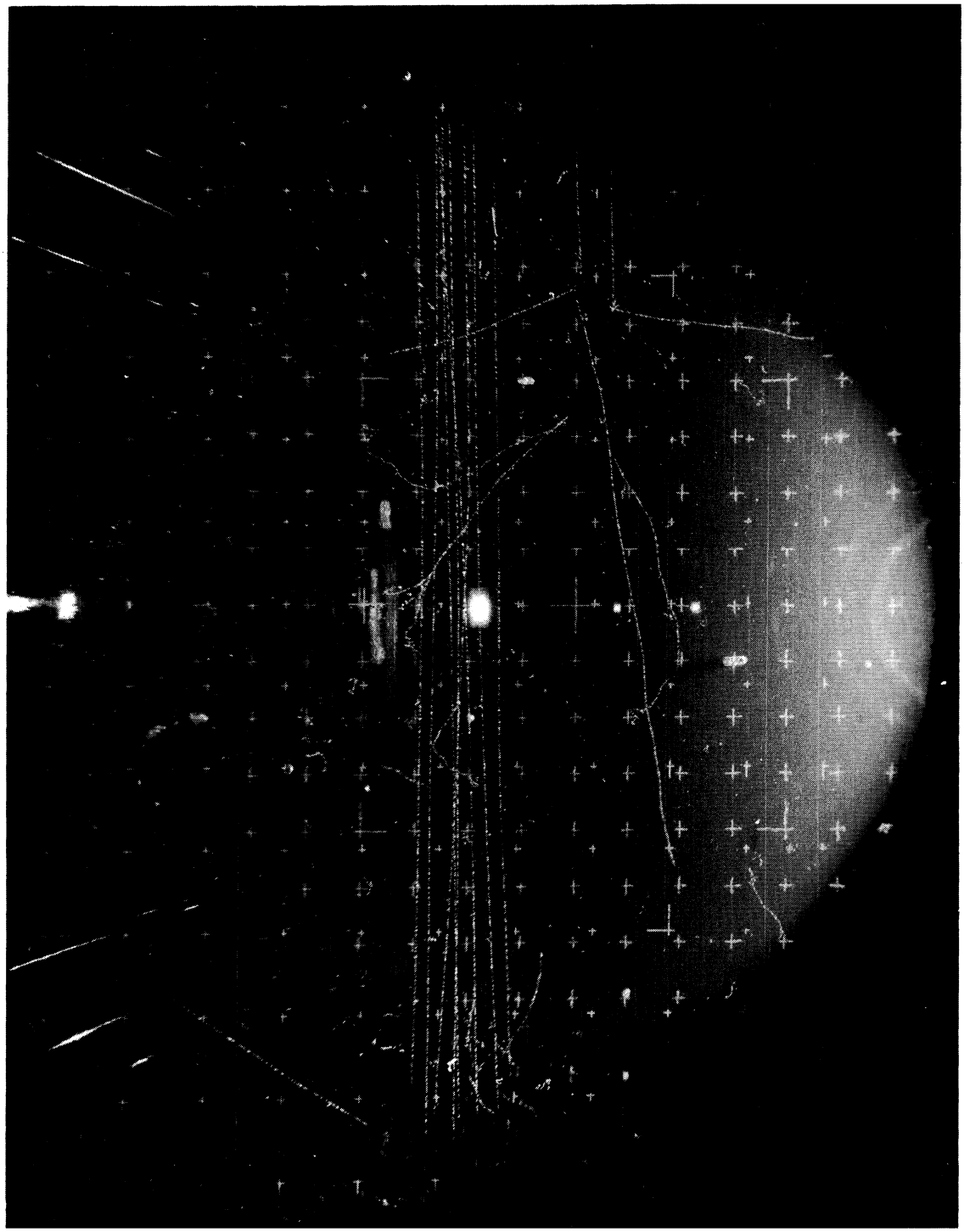

Fig. 5. Single K_1^o with Two Associated Gamma Rays.

Table 3. The Computed Results of a Measurement of the Event Shown in Figure 4

Spatial Coordinates (all measurements are in cm. unless otherwise indicated)

Point	x	y	z	Point	x	y	z
1	0.00	0.00	0.00	7	- 8.26	3.69	8.60
2	- 9.26	3.82	8.05	8	9.17	3.75	24.96
3	-10.53	3.76	8.02	9	- 4.28	4.20	11.22
4	- 8.80	3.67	7.84	10	- 3.95	4.36	11.33
5	- 8.21	3.10	6.36	11	- 5.54	2.76	11.15
6	- 6.10	0.62	0.09	12	- 5.23	2.25	11.52

Origin Data

Distance between 3 and 2 = 1.3

Direction cosines of the beam = 0.9988, 0.0447, 0.0177

V Data

Leg One: Range = 8.76 = 1.69 + 7.07
Chord (distance between 4 and 6) = 8.8
Angle between two segments of leg one = 3.4°
Direction cosines of leg one = 0.3534, -0.3359, -0.8731

Leg Two: Range = 24.85 = 0.93 + 23.91
Chord = 24.8
Angle = 11.3°
Direction cosines of leg two = 0.5820, 0.0266, 0.8128

Opening Angle (angle between the two legs of the V), θ = 120.9°
Errors in θ due to motion of the dependent coordinates by 100 microns:
4) 3.9°, 1.6°, 1.0°
5) 1.5°, 0.3°, 0.7°
7) 2.3°, 1.1°, 1.6°

V Origin Data

Direction cosines of the V = 0.8733, -0.2957, -0.3872

Decay Length = 0.53

Potential path = 15.61

Production angle = 31.5°

Direction cosines of normal to the production plane = -0.0230, 0.7687, -0.6391

Table 3. V Origin Data (con't)

Angle between leg one and the V direction, θ_1 = 79.3°
Errors in θ_1 due to motion of the coordinates by 100 microns:
2) 2.5°, 0.5°, 4.7°
4) 0.3°, 1.1°, 6.8°
7) 2.3°, 1.9°, 1.6°

Coplanarity angle, δ = 4.2°
Errors in δ due to motion of coordinates by 100 microns:
2) 1.4°, 5.0°, 1.1°
4) 2.5°, 9.2°, 2.3°
5) 0.5°, 1.8°, 0.5°
7) 0.7°, 2.2°, 0.6°

Gamma Ray Data

Distance one must move coordinates of 12) if gamma one were to come from origin = 0.22, 0.36, 0.07

Distance one must move coordinates of 10) if gamma two were to come from origin = -0.01, -0.13, 0.09

Length of nose of gamma one (distance between 11 and 12) = 0.71

Length of nose of gamma two (distance between 9 and 10) = 0.37

Coordinates of best origin point : -5.95, 3.43, 10.66

Distance of closest approach of the projected paths of the gammas = 0.006

Conversion length of gamma one = 0.92

Conversion length of gamma two = 1.92

Amounts one must add to coordinates of 12) if gamma one were to come from best origin point:
0.000, 0.000, 0.000

Amounts one must add to coordinates of 10) if gamma two were to come from best origin point:
.001, .000, .001

Production angle of parent = 38.0°

Decay length = 4.23

Angle between gammas = 75.9°

the V from the origin, θ_1 and θ_2, and the distances the two legs go in the chamber, R_1 and R_2. If a track does not leave the chamber it is not always clear whether it stops or interacts, although bubble density is a clue. This ambiguity must always be kept in mind. One starts by making a reasonable assumption about the fate of each leg.

1) If both legs stop in the chamber the V cannot be a K_1° (except under rare circumstances). Then assuming the V is a lambda one uses the two ranges R_1 and R_2 to determine the predicted opening angle, θ, for which there are in general two possibilities depending on which leg is chosen as the proton. By comparing θ as predicted and θ as measured one then tentatively decides if the V is a lambda and which leg is the proton. If the V is consistent with being a lambda then the predicted opening angle, θ, and the range of the proton or the range of the pion are used to predict the angle between the line of flight of the V and the proton or pion, θ_p or θ_π. If the predicted angles, θ_p and θ_π, are consistent with their counterparts, θ_1 and θ_2, and the coplanarity angle, δ, is consistent with being zero, then the V is identified as being a real Λ to origin. If θ is consistent, but δ and θ_1 and θ_2 are not, then the V is identified as a possible scattered Λ. The predicted angles, θ_p and θ_π, are used to determine the momentum and the center of mass decay angle for the Λ. If θ is not consistent, but δ is consistent with being zero, one side may not have actually stopped, and one proceeds to 2).

2) If one side stops, say leg 1, and δ is consistent with being zero, one uses R_1 and θ to predict θ_1 under the assumptions that a) the V is a K_1°, b) the V is a Λ with leg 1 as proton and c) the V is a Λ with leg 1 as pion. If none of these assumptions gives a prediction for θ_1 that

is consistent with its measured value, the one proceeds to 3). If one or more of these assumptions give a consistent value for θ_1 then one uses $\theta_2 = (\theta - \theta_1)$ to predict a range for leg 2. If this predicted range is significantly less than the measured lower limit on the range then one proceeds to 3). If not, one may be able to decide further between the assumptions a), b) or c) if there were any ambiguity. One then uses the predicted angles θ_1 and θ_2 to determine the momentum and the center of mass decay angle. It is not always possible to differentiate by the above means between a lambda and a K°_1, however, and further information must be used such as bubble density and the identity of the other particle in the picture if there is another particle associated.

3) If neither side stops and the coplanarity is consistent with zero, then one uses the two angles, θ_1 and θ_2, to predict the ranges of the two legs. By comparing the predicted ranges with the lower limits on the ranges as measured, R_1 and R_2, one can eliminate bogus V's and usually differentiate between Λ's and K°_1's, although this is not always possible. If the ranges are consistent with the measurements, one uses the two angles to determine the momentum and the CM decay angle.

The analysis and computations of associated pairs

As described above each electron pair believed to be associated with a suspected K°_1 and one or more other such pairs was measured at two points, one being the apex and the other point the most representative in the opinion of the measurer of the most likely direction of the gamma ray. As pointed out above usually the second point is chosen where the two electron tracks of the pair appear to diverge from each other, although there are many exceptions for the cases when the energy is very unequally divided

between the two electrons or when, as in the case of pairs nearly perpendicular to the beam direction (x-axis), it is more important that one be assured he is measuring corresponding points. (The difference between the x coordinates of two points is practically constant for the two stereo views, but the y difference is not.)

Then from the positions and directions of any two electron pairs one computes the most likely point of origin of their two parent gamma rays, this point being defined as the point for which the quantity

$$Q = \Delta_1^2 + \Delta_2^2$$

is minimized where Δ_k is the distance one must move the second point of the measurement of the k^{th} gamma ray in order that the projected path of the gamma ray pass through the hypothesized point of origin.

From the best meeting point one calculates the production angle of the Λ, assuming it is from the same origin as the K_1°, and also its decay distance, L_Λ.

One can estimate a lower limit on the energy of each pair by measuring the total length of the electron paths of each pair. This was done by tracing the paths on both views with a "verstmeter", a small roller device used to measure distances on maps, and using a scaling factor given by the calculated distance between two measured points and the same distance as measured with the verstmeter. The energy loss per centimeter by minimum ionizing particles is about 2.79 Mev in the bubble chamber. This was taken to be the energy loss of the electrons, neglecting such effects as relativistic rise.

IV. NEUTRAL PIONIC BRANCHING RATIO OF THE Λ

Definitions of the problem

As described in the preceeding chapter the rough data for the calculation of the branching ratio, B_Λ, consists of all events of the type

$$\pi^- + \text{xenon nucleus} \longrightarrow \Lambda + K^\circ + \text{residuals}$$

or

$$\longrightarrow \Sigma^\circ + K^\circ + \text{residuals}$$

where $\Sigma^\circ \longrightarrow \gamma + \Lambda$ (lifetime 10^{-19} seconds)

for which the Λ decays either as

i. $\Lambda \longrightarrow \pi^- + p^+$

ii. $\Lambda \longrightarrow \pi^\circ + n$

and the K° appears as a K_1° and decays as

$$K_1^\circ \longrightarrow \pi^+ + \pi^-$$

Operationally we can define the two categories as

i.) A V with an origin that satisfies the kinematics conditions on $K_1^\circ \longrightarrow \pi^+ + \pi^-$ (see analysis of V's, page 15) and another V which satisfies the kinematics conditions on the decay $\Lambda \longrightarrow \pi^- + p$ and which could have been produced at the same interaction from which the K_1° appears to come.

ii.) A V with an origin that satisfies the kinematics conditions on $K_1^\circ \longrightarrow \pi^+ + \pi^-$, and at least two associated electron pairs.

From these two categories of rough data two final data categories

were chosen according to the criteria stated below. We shall denote these two final categories as ABC (corresponding to i) and ABD (corresponding to ii). The criteria were chosen to insure high scanning efficiency and to cut down on background events.

Before the numbers of events found to be in the two categories ABC and ABD can be compared several corrections must be made. These corrections are listed below with their corresponding correction factors, σ. It is important to note at this point that no biases affecting the branching ratio are introduced by the criteria on K_1° since the K_1° is simply used as a "signature" for the presence of a Λ.

We define the ratio of neutral to charged events to be

$$R = \frac{w(\Lambda \longrightarrow \pi^\circ + n)}{w(\Lambda \longrightarrow \pi^- + p)}$$

and experimentally

$$R = \frac{\sigma_1 \sigma_2 \sigma_3 ABD}{\sigma_4 \sigma_5 \sigma_6 ABC}$$

where ABD and ABC are taken to stand for the number of events found in the corresponding categories, and where

σ_1 is the correction for the fact that not all occurrences of neutral decay have both gammas converting in the chamber.

σ_2 is the correction for events that satisfy ABD but are really cases in which only one gamma from the π° converts, the other gamma coming from the decay of a Σ°.

σ_3 is the correction for background in the ABD category.

σ_4 is the correction for the bias introduced by restriction C_3 below (cutoff).

σ_5 is the correction for the bias introduced by restriction C_5

below (one-legged V's).

σ_6 is the correction for the relative scanning efficiency for the ABC events compared to the ABD events.

The branching ratio as defined above then will be given by

$$B_\Lambda = \frac{R}{1 + R} .$$

Criteria

A. General

1. The picture must have less than 16 beam tracks. A beam track is defined as any lightly ionized track entering the chamber at a projected angle on either view less than 15° with respect to the x (beam) axis.
2. The picture must have no background of bubbles or electron showers which could possibly obscure an electron pair, or less likely, a V.
3. The picture may not be torn, badly developed or damaged in any way.
4. The presumed origin for the associated particles satisfying the criteria below must not have a prong that leaves the chamber. (This requirement was used in part II to eliminate many useless measurements of bogus V's but very few good ones.)

B. Restrictions on the K_1°

1. There must be a V in the picture that fits the kinematics curves for the two-body decay of the K_1° within the expected errors, and for which the predicted ranges are in agreement with their observed bubble densities.
2. The measured coplanarity δ of the V from the first measurement must be less than or equal to five degrees, independent of the

estimated errors involved. (Since K_1° with wide opening angles have in general larger errors than K_1° with small opening angles, wide-angle K_1°'s are discriminated against here. This discrimination is desirable here because the wide angle V's are difficult to recognize and hence their detection depends on the detection of the lambda.)

3. The decay distance must be at least 5 millimeters.
4. The apex of the V must fall within the fiducial volume defined by $R \leq 11$ centimeters ($R^2 = x^2 + y^2$); 2 cm. $\leq z \leq$ 24 cm.

C. Requirements on the charged mode

1. In addtion to the K_1° there must be a V in the picture that fits the kinematics curves of the lambda within the expected errors and for which the bubble densities are consistent with the predicted ranges.
2. The V, although it may have scattered, must be consistent with having been produced at the same origin as the V satisfying criteria B above.
3. The decay distance must be at least 5 millimeters.
4. The apex must fall within the fiducial volume defined in B3 above.
5. Both legs of the V must be greater than 2 millimeters in length.

D. Requirements on the neutral mode

1. There must be at least two electron pairs in the picture that are consistent with having been produced by gammas having a common origin.
2. Neither of the pairs must appear to have come from an interaction, excluding the production reaction.
3. Each pair must have at least 3 centimeters of electron track.

4. The apex of each pair must fall inside the fiducial volume defined in B3 above.

Uncorrected results:

Events satisfying ABC in part I, 51. In part II, 45.

Events satisfying ABD in part I, 15. In part II, 20.

Events satisfying ABCD in part I, 1. In part II, 0.

The distribution in δ for the K_1°'s in the ABC and ABD categories and for the Λ's in the ABC category can be seen in Fig. 6. The difference between the measured opening angle, Θ, and the predicted opening angle, Θ', (based on the ranges of the two legs) for all ABC Λ's for which both legs stop in the chamber without suffering any apparent inelastic collisions can be seen in Fig. 7. (Of the 96 ABC Λ's, 51 have both legs stop, 33 have only one leg stop, and 12 have neither leg stop.) Other properties of interest of ABC and ABD events are tabulated in Appendix E.

Corrections

A. The neutral mode

1. The conversion probability for both gammas from the π° is the largest correction made and was based on a Monte Carlo calculation. In effect this calculation computed the average probability for conversion for a sample of π°'s having the same momenta and positions as a group of π^-'s from lambdas occurring in double V events. The events chosen were required to pass A3 and A4, and B and C, except C3 and C5. The calculation was performed on the IBM 704.

The input data for each event were i) the size of the fiducial volume as defined in B4, ii) the location of the lambda apex, iii) the energy of the pion as obtained from its measured or calculated range, iv) the direction cosines of the pion. The calculation went as follows: The pion was allowed

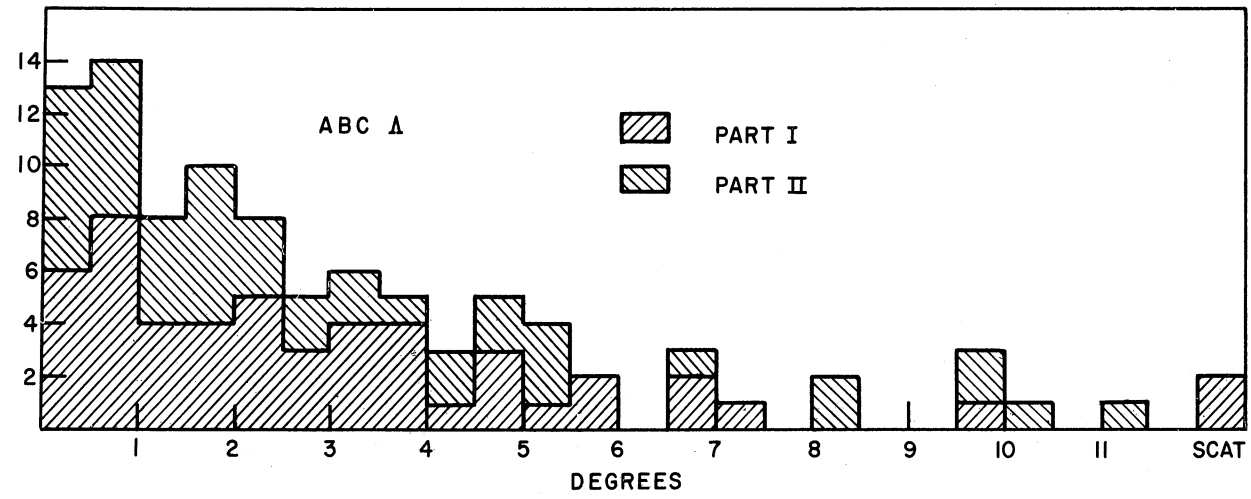

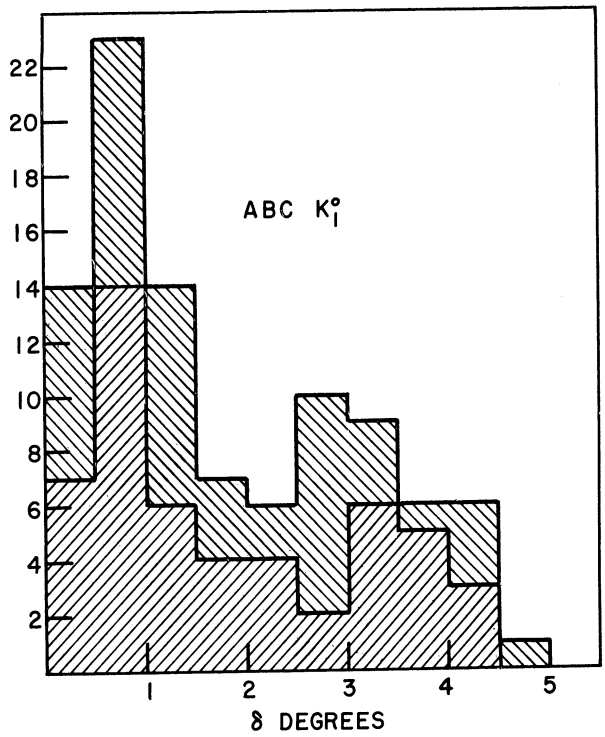

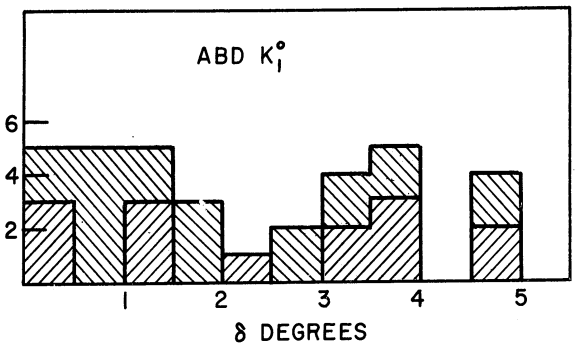

Fig. 6. Distribution of δ for K°_1's and for Λ's.

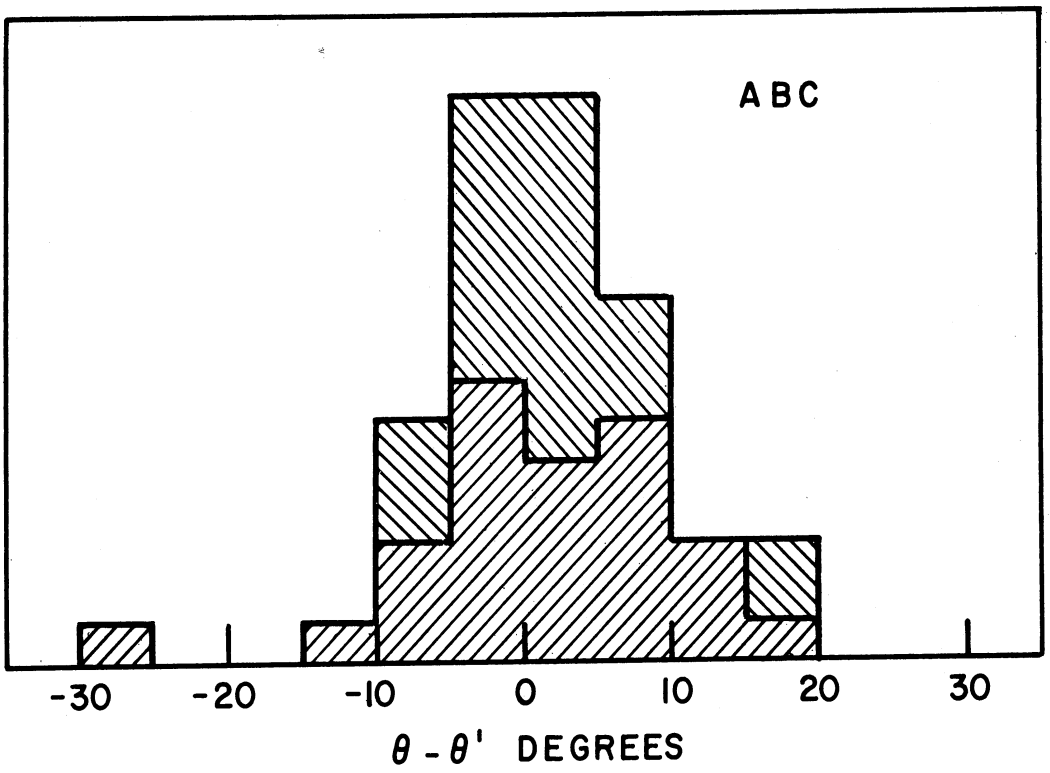

Fig. 7. Distribution of Difference between Measured θ and Predicted θ' for Λ's with Both Sides Stopping.

to decay using five different sets of center-of-mass decay angles based on 10 random numbers generated by a computer subroutine. For each of the resulting hypothetical gamma rays a potential path was computed and the probability that the gamma would convert within the potential path was computed using a relation between mean conversion distance and energy discussed below. Then using the results for the five trials the probabilities of one and two gammas converting in the chamber were computed. The average conversion probability for the sample was then obtained.

The results of this calculation gave the following where the errors quoted are statistical:

Probability that both gammas convert (denote P(2))

Part I $P(2) = .48 \pm .02$

Part II $P(2) = .51 \pm .02$

Probability that only one of the gammas convert (denote P(1))

Part I $P(1) = .43 \pm .01$

Part II $P(1) = .40 \pm .01$

The correction factor, σ_1, defined on page for conversion probability is then

$$\sigma_1 = 2.02 \pm 0.04$$

The relation between mean conversion length, λ in centimeters, and the gamma energy, E_g in Mev, used in the Monte Carlo calculation was

$$\lambda = 5.09 + \frac{157.2}{E_g} - \frac{170.0}{E_g^2}$$

This formula was got by empirically fitting the results of a numerical integration on the Bethe-Heitler formula with corrections for screening, use of the Born approximation, and production in the electron's field (15).

The density of xenon was taken to be 2.167 gm./cm.^{3}. The results which the formula is taken to represent are below.

E_g (Mev)	λ (cm.)
10	19.10
30	9.868
50	8.165
70	7.391
100	6.826
200	6.042
500	5.627
∞	5.090

One can show from the calculated energy distribution for converted gamma pairs by the Monte Carlo method given in Fig. 8 that the use of the above empirically fit formula gives an estimate of the conversion efficiency which is about 1% too high. This effect has been neglected.

2. Correction for Σ° events. Certain of the events satisfying criteria ABD were not really cases in which both gammas from the π° converted, but rather cases in which only one gamma from the π° converted and the gamma from a Σ° also converted. Since gammas from Σ° occur in about 10% of the double V events, 10% of the cases where only one gamma from the Λ converts appear as 2-gamma events. In some cases these events are consistent with identification as bona fide neutral decay events, i.e. they satisfy D.

The correction for this effect was made as follows. All events that satisfied ABD and which had three associated gamma ray pairs were examined carefully. Let us denote the three pairs as a, b, and c. If all three of combinations ab, ac, and bc could be mistaken for gammas from the lambda then the event is assigned the number 1. If only two of

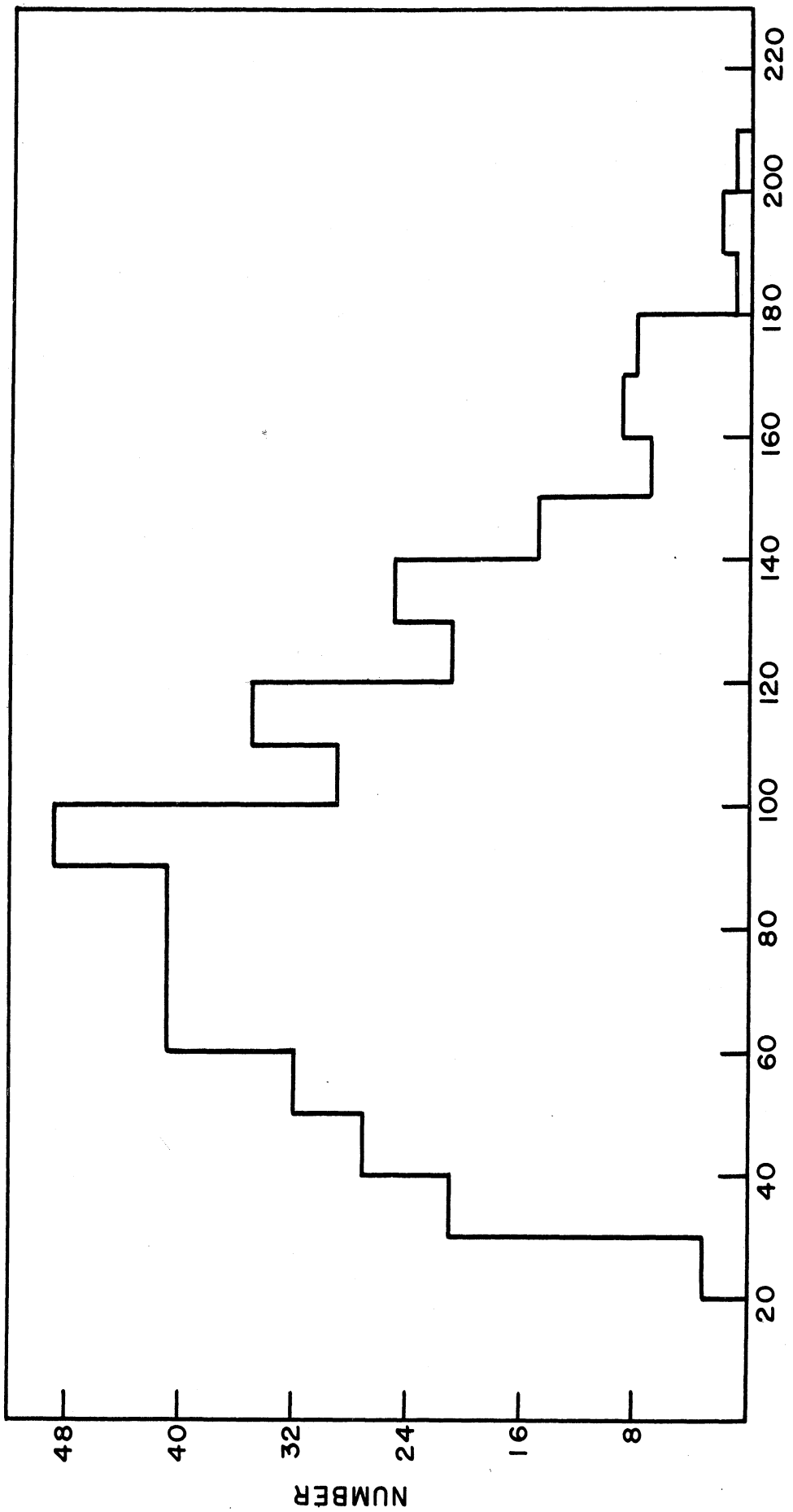

Fig. 8. Calculated Energy Distribution for Converted Gamma Pairs.

the combinations could be mistaken for the gammas from the lambda then the event is assigned the number 1/2. If only one of the combinations could be real, then the event is not counted. Then one expects that the number of bogus two-gamma events in the sample will be the sum of the assigned numbers multiplied by the ratio of the probability of one gamma converting to the probability for two gammas converting.

In part I two such three gamma events were found each with weight 1. In part II two such events were found, each with weight 1/2. The total correction will then be

$$2x \frac{.43}{.48} + \frac{.40}{.51} = 2.6 \text{ events.}$$

The correction factor then for ABD events will be

$$\sigma_2 = .93 \pm .04$$

where the error is statistical.

3. Background. In the 96 events satisfying ABC, one event was found that also satisfied criteria D. This means that the background of events satisfying D is about 1%, or

$$\sigma_3 = .99 \pm .01.$$

4. Correction for electron pairs for which the electron track length is less than 3 cm., i.e. those that fail D3.

R.R. Wilson (16) has made some Monte Carlo calculations on the range and straggling of electrons in lead. His results were stated in terms of radiation lengths and should apply in general. He finds the following equations describe his results

$$R(E) = l_r \ln 2 \ln (E/\beta \ln 2 + 1)$$

where R(E) is the range in centimeters of an electron of energy E in Mev, l_r is the radiation length in centimeters, β is the energy lost by an electron going one radiation length (minimum ionizing) in Mev. For xenon l_r = 3.9 cm. and β = 10.88 Mev.

The percentage straggling (RMS) is given by S/R(E) where

$$S/R(E) = (1 - \beta R(E)/l_r E) (\ln 2\, l_r/R(E))^{1/2}$$

These results do not take into account multiple scattering.

As an estimate of the ranges of electrons occurring in pairs in the xenon chamber we took the average range of the two extremes, namely when the energy of the gamma is equally divided between the two electrons and when one electron takes all the energy of the gamma. The probability for any particular ratio of energies is roughly independent of the ratio. That is we took as the range of the pair

$$R_{pair} = \frac{R(E) + 2R(E/2)}{2}$$

where E is the energy of the gamma producing the pair. The straggling was taken as

$$S_{pair} = \frac{(S(E)^2 + 4S(E/2)^2)^{1/2}}{2}$$

The results of this are

E_{pair}	R_{pair}	S_{pair}	% less than 3 cm.
20 Mev	4.03 cm.	1.20 cm.	20.0
30	5.14	1.62	9.0
40	5.99	1.96	6.5
50	6.69	2.25	5.0
60	7.28	2.50	4.5
80	8.21	2.88	3.5
100	9.06	3.20	3.0
120	9.65	3.42	2.5
160	10.67	3.80	2.0
200	11.61	4.09	2.0

From the energy distribution of Monte Carlo gammas given in Fig. 8, one finds that about 3.5% of the gammas would be less than 3 cm. in length. This result should be regarded as an upper limit because it neglects secondary electrons, which in practice cannot be separated from the primaries. No correction was made therefore for pairs falling below 3 cm. in length. This requirement was responsible for the rejection of at least one event which satisfied the ABD conditions otherwise. The measured length of the rejected electron pair was 1.2 cm. This requirement of minimum track length was useful in that it eliminated the necessity for considering the numerous short background electron tracks that occur in the xenon chamber.

B. The charged mode

1. Correction for lambdas decaying less than 5 mm. from their origins. There is no restriction corresponding to the 5 mm. decay length cut-off (C3) for the charged mode placed on the neutral mode. In order to correct for this we must calculate the ratio of decays occurring from 0 to 5 mm. compared to the number occurring from 5 mm. to the potential paths. We

take the probability for decay at a distance x from the origin in an interval dx as

$$P(x)dx = (1/\lambda) \exp(-x/\lambda)\, dx$$

where λ is the mean decay length and is given by

$$\lambda = p\tau c/m$$

where p is the momentum of the lambda in Mev/c, m is the rest energy in Mev (1115.2), τ is the lifetime in seconds (2.50×10^{-10}) and c is the velocity of light in cm./sec.

Then for N events found to fit the criteria one expects the number missed from 0 to 5 mm. will be n where

$$n = \sum_{i=1}^{N} \frac{1 - \exp(-.5/\lambda_i)}{\exp(-.5/\lambda_i) - \exp(-l_i/\lambda_i)}$$

where l_i is the potential path of the lambda in event i.

The quantity n/N was computed using the 84 ABC events with origins inside the fiducial volume (see page 27) and was found to be

$$n/N = .214 \pm .011, \text{ where the error is statistical.}$$

The correction for ABC events is then

$$\sigma_4 = 1.214 \pm .011.$$

2. Correction for one legged Λ's. One legged Λ's are those cases of the charged mode in which one of the two legs is too short to be seen. Because one legged events might be overlooked and, if found, are difficult to identify positively, the requirement that both legs have ranges longer than 2 mm. (C5) was imposed on the ABC events

and a correction made for those failing this requirement:

Let E_p, E_p^* and P^* be the total energy in the LAB, total energy in the Λ CM and momentum in the Λ CM, respectively, of the proton, and E_π, E_π^* and P^* be the corresponding quantities for the π. Then

$$E_p = \gamma (E_p^* + \beta P^* \cos \Theta^*)$$

and

$$E_\pi = \gamma (E_\pi^* - \beta P^* \cos \Theta^*)$$

where $\beta = v/c$ where v is the velocity of the Λ and

$$\gamma = (1 - \beta^2)^{-1/2}$$

and Θ^* is the angle between the proton and the Λ line-of-flight in the Λ CM.

Putting in numerical values and letting the energies of the π and p corresponding to range of 2 mm. be E_π(2 mm.) and E_p(2 mm.) respectively one can show that it is possible for $E_p < E_p$(2 mm.) only for the Λ momentum, P_Λ, less than 308 Mev/c and $E_\pi < E_\pi$(2 mm.) for $400 < P_\Lambda < 1200$ Mev/c.

Let us designate the % of Λ's with both legs greater than 2 mm. by $F(P_\Lambda)$, a function of the Λ momentum. Then for

$$P_\Lambda < 67 \text{ Mev/c}, \quad F(P_\Lambda) = 0.$$

For

$$67 < P_\Lambda < 308 \text{ Mev/c},$$

$$F(P_\Lambda) = \frac{1 - \cos \Theta^* \text{ (2 mm.)}}{2}$$

where

$$\cos \Theta^*(2 \text{ mm.}) = \frac{E_p(2 \text{ mm.}) - \gamma E_p^*}{\beta\gamma P^*}$$

and $E_p(2 \text{ mm.}) = 951.2$ Mev; $E_p^* = 943.5$; $P^* = 99.4$ Mev/c.

For $308 < P_\Lambda < 400$ Mev/c, $F(P_\Lambda) = 100\%$.

For $400 < P_\Lambda < 1200$ Mev/c,

$$F(P_\Lambda) = \frac{1 + \cos \Theta^*(2 \text{ mm.})}{2}$$

where

$$\cos \Theta^*(2 \text{ mm.}) = \frac{\gamma E_\pi^* - E_\pi(2 \text{ mm.})}{\beta\gamma P^*}$$

where $E_\pi^* = 171.7$ Mev; $E_\pi(2 \text{ mm.}) = 146$ Mev; $P^* = 99.4$ Mev/c.

For $P_\Lambda > 1200$ Mev/c, $F(P_\Lambda) = 100\%$.

A plot of $F(P_\Lambda)$ as a function of P_Λ is given in Fig. 9.

The correction factor then, as defined on page is

$$\sigma_5 = 1/N \sum_{i=1}^{N} 1/F(P_{\Lambda i})$$

where $P_{\Lambda i}$ is the momentum of the i^{th} Λ.

Using 94 ABC events (the two Λ's that clearly scattered were omitted)

$$\sigma_5 = 1.069 \pm .011, \text{ where the error is statistical.}$$

C. Scanning efficiency

1. The direct method for determining scanning efficiency is to scan some number of frames twice, say by scanners 1 and 2.

Let n_3 be the number of events found by both scanners, n_1 be the number found by 1 alone and n_2 be the number found be scanner 2 alone. Then the "true" number of events in the sample should be

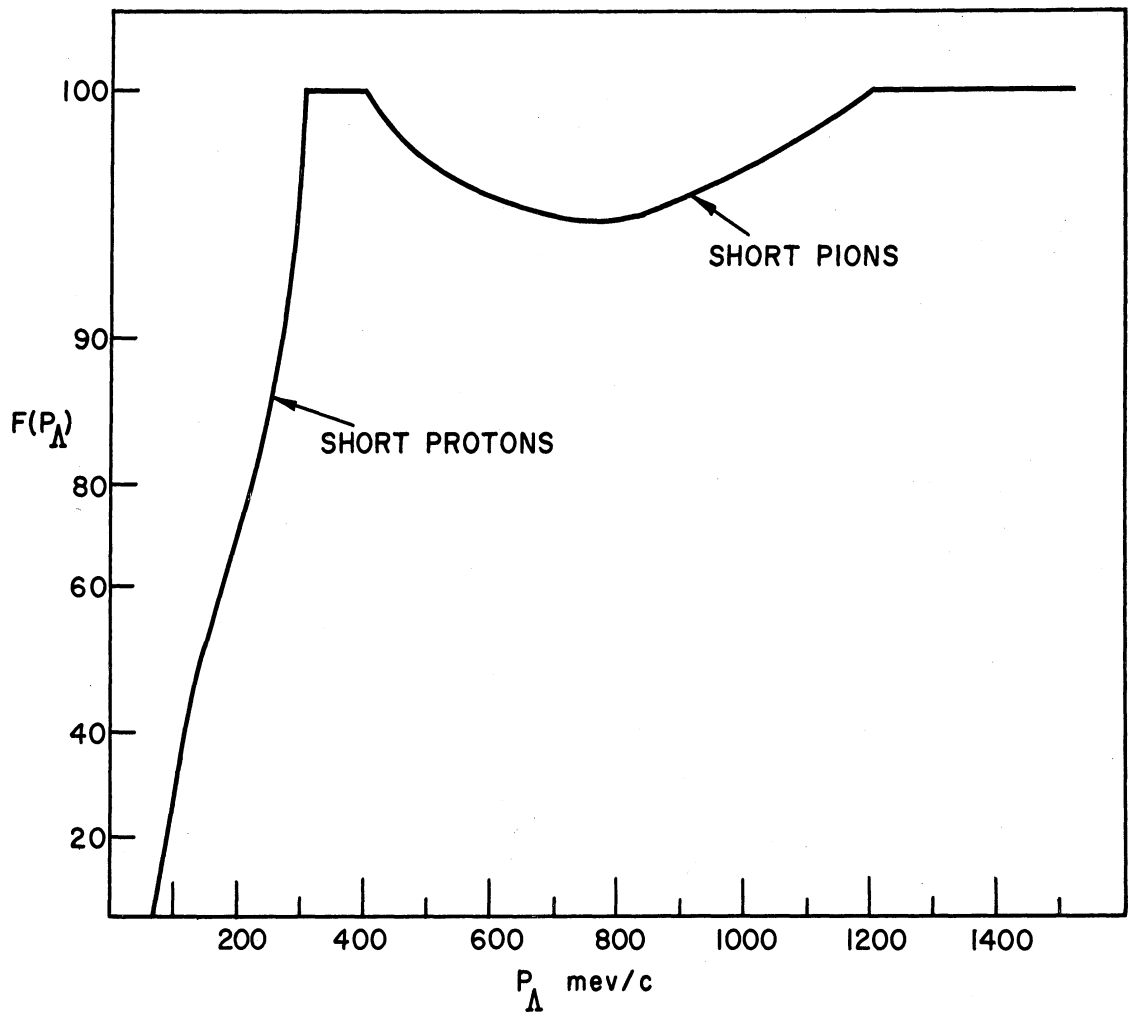

Fig. 9. The Percentage of Λ's with Legs Less than 2 mm Versus P_Λ.

$$N = \frac{n_1 + n_2 + n_3}{(1 - (1-x)(1-y))}$$

where x is the scanning efficiency of 1 and y is the scanning efficiency of 2, and assuming x and y are independent.

So

$$x = \frac{n_3 + n_1}{N} \qquad \text{and} \qquad y = \frac{n_3 + n_2}{N}$$

Solving for N we get

$$N = \frac{(n_3 + n_2)\,(n_3 + n_1)}{n_3} .$$

The results of rescanning

	criteria satisfied	n_3	n_2	n_1	x	y	N
Part I	ABC	5	0	0	1	1	5
	ABD	2	1	0	5/6	1	6
	AB only	4	0	0			
Part II	ABC	14	0	0	1	1	14
	ABD	6	0	0	1	1	6
TOTAL	ABC	19	0	0	1	1	19
	AB only and ABD	12	1	0	12/13	1	13

From this data we estimate the relative scanning efficiency for ABD events compared to ABC events is 0.96 ± 0.07.

2. Another estimate of the relative scanning efficiency of the ABD events compared to ABC events can be made by assuming

i. The gamma rays do not aid in the finding of ABD events.

ii. After an event has been located by the scanner he does not look for additional V's in the picture.

iii. The measuring and additional film-handling always turn up all V's on frames designated by the scanners as containing events of interest.

Then the relative scanning efficiency can be obtained from the number of events in the ABC category that were originally identified as AC events, i.e. the K_1° was not seen by the scanner. There were two such events out of the 51 in part I and 2 out of 45 in part II. The relative scanning efficiency is therefore on this basis 92/96 or

$$0.96 \pm 0.02.$$

Since this estimate makes some unjustified assumptions about the psychology of scanning, it should be taken only with reservations.

3. One expects that the major scanning biases, if there are any, should appear when distributions of the events in the variables that influence the visibility of the events are studied. One might expect that the two most accessible variables to affect the scanning efficiency would be

i. The number of beam tracks per picture, since the amount of background in the picture should be roughly proportional to the number of beam tracks, and

ii. The center-of-mass decay angle of the K_1°, since the opening

angle of the K_1° as well as the distribution of momenta between the two legs should affect the visibility of the K_1° and these two characteristics depend on the center-of-mass decay angle. The decay of the K_1° should be isotropic in the center-of-mass decay angle since the K_1° has no spin.

Let us see then if any useful information can be obtained from looking at the distributions in these two variables.

i. The number of tracks per picture.

Let us take the relative scanning efficiency for ABD events with respect to ABC events as being linearly dependent on the number of tracks per picture, and being unity when there are no beam tracks per picture.

That is, we take

$$e(x) = 1 - ax$$

where $e(x)$ is the relative scanning efficiency as a function of x, the number of tracks per picture. The average scanning efficiency for ABD events compared to ABC events is then

$$a = \frac{\bar{x}_o - \bar{x}}{\bar{x}_o \bar{x} - \overline{x^2}}$$

where $\bar{x}_o$ is the average of x over the ABD sample and $\bar{x}$ and $\overline{x^2}$ are over the ABC sample. These two distributions are shown in Fig. 10.

We find

$$\sigma_x = 1.15 \pm 0.55.$$

This method is therefore much too inaccurate to be of use.

ii. The center-of-mass decay angle.

Let the cosine of this angle be given by y. Assume that the

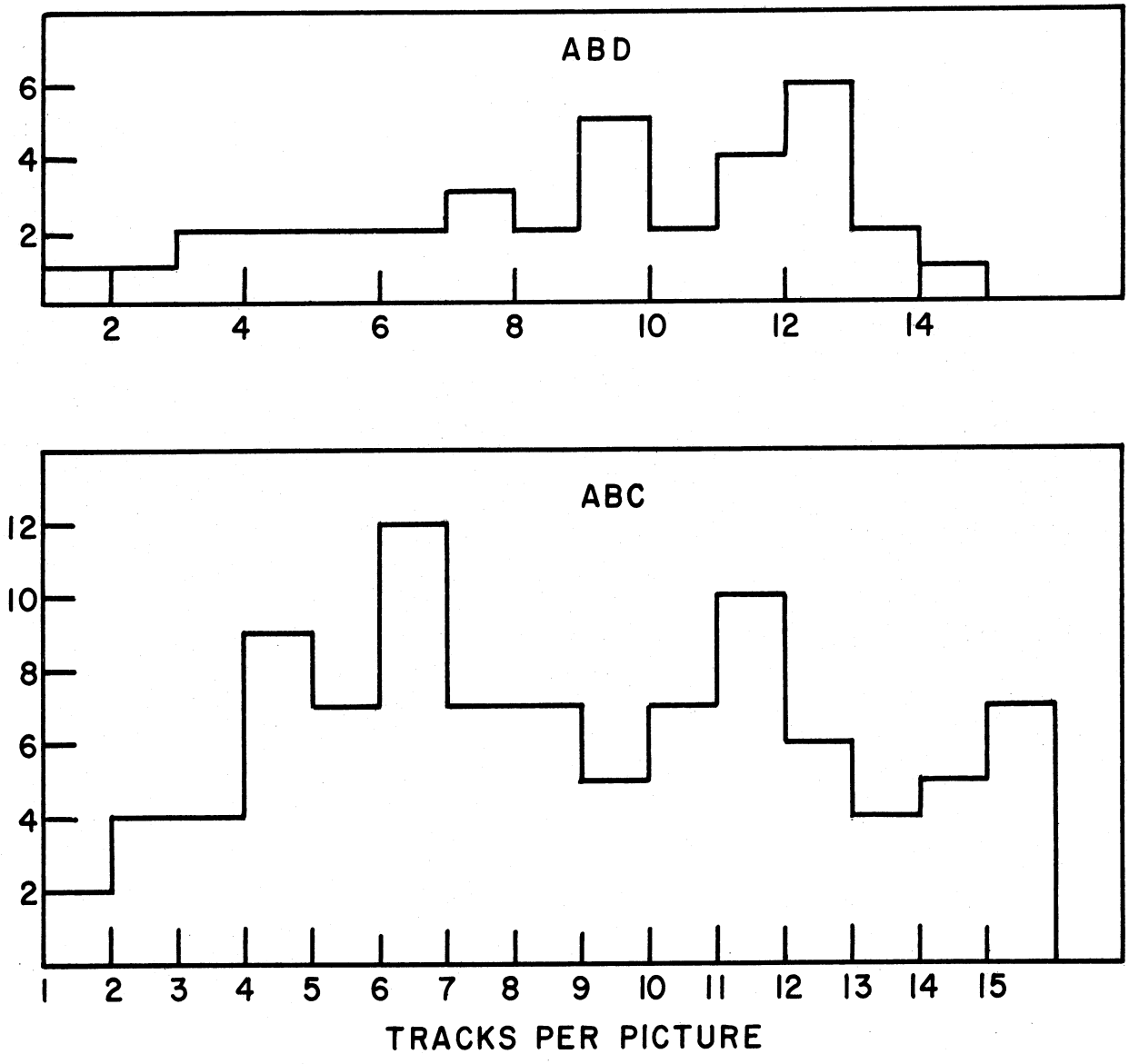

Fig. 10. Distributions of the Number of Tracks Per Picture Versus Number of Pictures.

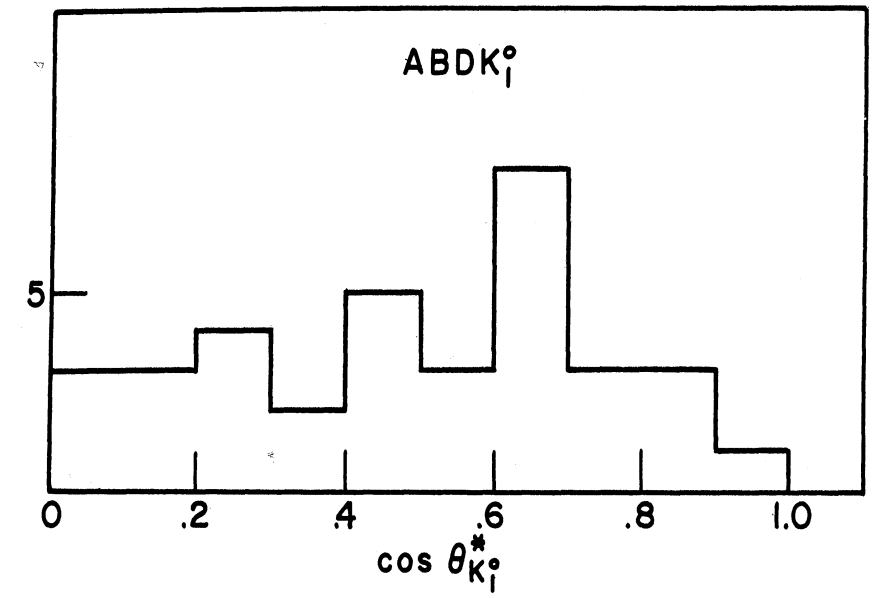

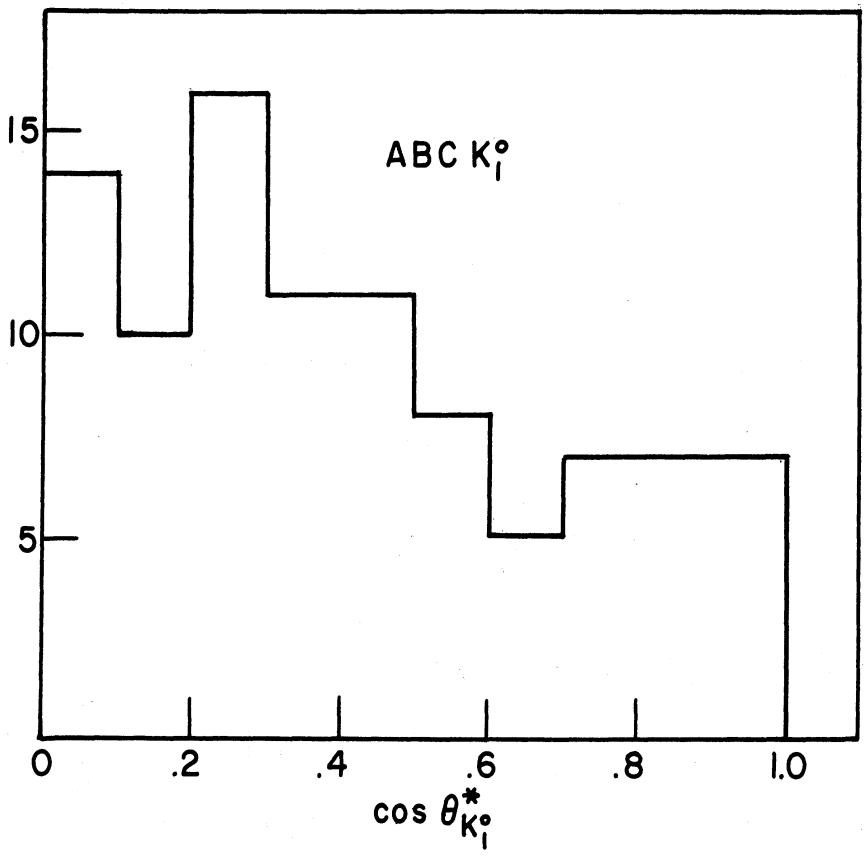

Fig. 11. Distributions of Cos $\Theta^*_{K^\circ}$.

dependence on y of the scanning efficiency is given by

$$e(x) = 1 - by^2$$

b is then given by

$$b = \frac{\bar{y}_o - \bar{y}}{\bar{y^2}\bar{y}_o - \bar{y^3}}$$

The distribution of y in the two categories is given in Fig. 11. We find

$\sigma_y = \overline{e(y)} = 1.24$, where the statistical error due to $\bar{y}_o$ alone is $\pm$ 0.24. Thus this method also is too imprecise to be of use.

Conclusion: The relative scanning efficiency will be taken as that given by the direct rescan, namely

$$\sigma_6 = 0.96 \pm 0.07$$

Results of the calculations:

As the result of the foregoing considerations we have the following values for the constituents of the equation

$$R = \frac{\sigma_1\sigma_2\sigma_3}{\sigma_4\sigma_5\sigma_6} \quad \frac{ABD}{ABC} :$$

ABD/ABC = 35/96 = .364 $\pm$ .072

$\sigma_1 = 2.02 \pm .04$ $\qquad$ $\sigma_4 = 1.214 \pm .011$

$\sigma_2 = .93 \pm .04$ $\qquad$ $\sigma_5 = 1.069 \pm .011$

$\sigma_3 = .99 \pm .01$ $\qquad$ $\sigma_6 = .96 \pm .07$

So

$$R = .54 \pm .12$$

and

$$B_\Lambda = \frac{R}{1 + R} = .35 \pm .05.$$

It is of interest to compare this number with (10)

$$\frac{w(\Lambda \rightarrow \pi^- + p)}{w(\Lambda \rightarrow \text{all modes})} = .627 \pm .031.$$

The fraction of Λ's decaying via pionic modes is then

$$(1 + R)\ \frac{w(\Lambda \rightarrow \pi^- + p)}{w(\Lambda \rightarrow \text{all modes})} = .966 \pm .089.$$

V. OTHER PROPERTIES OF THE Λ

A. The Asymmetry Parameter of the Λ.

In the Λ CM the angular distribution of the π is given by (see Appendix A)

$$\frac{dI}{d\Omega} = \frac{1}{4\pi}\left[1 + \alpha \bar{P} \cos \xi^*\right]$$

where ξ^* is the angle between the pion and the direction of polarization of the Λ, $\bar{P}$ is the average polarization of the Λ (averaged over all production angles), and α is given by (see Appendix A)

$$\alpha = \frac{2\,\mathrm{Re}\, S^* P}{S^* S + P^* P}$$

where S and P are the amplitudes of the L = 0 and L = 1 orbital angular momentum states occurring in the pionic decay of the Λ. These two states have even and odd parity, respectively. α therefore arises from the interference of two states of opposite parity.

The charged mode.

Because the Λ CM decay angle, $\theta^*_{\pi^-}$, of the π^- can be determined for the charged mode of the Λ (see page), it is possible to obtain the distribution of the π^- in the Λ CM from the observed distribution in the LAB. Since we assume parity conservation in the production of the Λ (see Appendix A), the polarization of the Λ is taken normal to the production plane. In this case ξ^* is related simply to the ξ in LAB by the formula

$$\cos \xi^* = \cos \xi \, \frac{\sin \theta^*}{\sin \theta_\pi}$$

where ξ is the LAB angle between the direction of polarization and the π^- line-of-flight, θ_π is the LAB angle between the Λ line-of-

flight and that of the π^-, and θ^* is the CM angle between the Λ line-of-flight and that of the π^- (or the proton).

The statistical estimate of $\alpha\bar{P}$ is got by using the distribution function

$$f(x, a) = \frac{1}{2}(1 + ax)$$

where we set $a = \alpha\bar{P}$ and $x = \cos\xi^*$. From $f(x,a)$ we construct the Bartlett "S-function" (17) which is given below

$$S(a) = \Delta a \sum_{r=1}^{N} \frac{\partial}{\partial a} \ln f(x_r, a)$$

where

$$\Delta a = \frac{1}{\sqrt{N}} \left[\int_{-1}^{+1} \frac{1}{f(x,a)} \left(\frac{\partial f}{\partial a}(x,a) \right)^2 dx \right]^{-1/2}$$

x_r is the value of $\cos\xi^*$ for the r^{th} event, and N is the number of events in the sample. For our case we may write therefore

$$S(a) = \frac{1}{\sqrt{N}} \left(\frac{2a^3}{\ln\left(\frac{1+a}{1-a}\right) - 2a} \right)^{1/2} \sum_{r=1}^{N} \frac{\cos\xi_r^*}{1 + a\cos\xi_r^*}$$

The most likely value of a (call it a_o) and the standard deviations on the plus and minus sides of a_o, Δa_+ and Δa_-, can be found from a graphical solution of the equations

$$S(a_o) = 0$$

and

$$S\left(a_o \begin{matrix} + \Delta a_+ \\ - \Delta a_- \end{matrix}\right) = \mp 1$$

A sample of Λ's was chosen from parts I and II to satisfy the following criteria:

1. The measurements of the Λ be in reasonable agreement with the kinematics graphs for the charged decay.

2. The coplanarity of the Λ, δ, be no greater than 7°.

3. The decay length of the Λ, L_Λ, be no less than 5 mm.

4. No origin prongs leave the visible volume of the chamber.

5. A possible K_1° charged decay occur in the picture which is consistent with having been produced with the Λ.

Any biases that may occur in the above sample are not expected to affect the measurement of the asymmetry. 222 events satisfied the above criteria and gave a result of

$$\alpha_- \overline{P} = +.32 \pm .11$$

The chance that an unpolarized sample give rise to this result is about 0.3%.

The neutral mode.

The most precise method for determining the asymmetry of the neutral mode is by looking at the distribution of the bisector in the CM of the angle between the two gammas from the π°, as discussed in Appendix B. Since the individual momenta of neutral events cannot be determined, the sample was assumed mono-energetic and transformed into the CM for several different values of the Λ momentum, P_Λ.

The sample was chosen to satisfy the criteria

1. No origin prongs leave the visible volume of the chamber.

2. A possible K_1° charged decay be associated with the event and be consistent with coming from the origin.

3. There be two gamma-produced electron pairs which are clearly associated with the event and whose directions are measurable.

Seventy-one events fell in the sample (from both parts) and

as shown below the dependence of the result on P_Λ was slight (for the charged mode the average P_Λ is about 500 Mev/c).

P_Λ(Mev/c)	$\pi/4\ w_B \alpha_0 \bar{P}$
0	$+.25 \pm .19$
300	$.25 \pm .19$
400	$.24 \pm .19$
500	$.24 \pm .19$
600	$.24 \pm .19$
700	$.23 \pm .18$

The factor w_B is a "washout factor" calculated in Appendix B where we show

$$w_B = 0.82$$

Therefore

$$\alpha_0 \bar{P} = +.37 \pm .28$$

As shown in Appendix A the ratio of asymmetry parameters for the two modes is of particular interest. Our result is not very meaningful, however. We find

$$\alpha_0/\alpha_- = +1.16 \pm .97$$

This quantity has been measured much more precisely by Cronin et al (12) using counters and was found to be

$$\alpha_0/\alpha_- = +1.10 \pm .27.$$

B. The lifetime of the Λ.

If the momenta and potential paths of a sample of Λ's is known in addition to their decay distances it is possible to estimate the lifetime. If in addition to requirements ABC in Chapter IV we require that

1. the origin be inside the fiducial volume of the two V's (see page 27),

2. the Λ charged mode be unscattered outside the nucleus,

we are left with a relatively unbiased sample from which a lifetime estimate can be obtained.

Using the Bartlett "S-function" corrected for skewness[17] we find for the 84 ABC Λ's that satisfy the above conditions

$$\Lambda \text{ Mean Life} = \left(2.77 \begin{smallmatrix} +.48 \\ -.34 \end{smallmatrix} \right) \times 10^{-10} \text{ seconds}$$

where the errors are standard deviations. The 5 mm. cut-off on the Λ decay distance (criterion C3 on page 27) has been taken into account.

Since the momenta of the neutral mode events cannot be determined no lifetime can be obtained directly for this mode. One can, however, compare the decay length distributions of the two samples, ABC and ABD, which are given in Fig. 12 . The following biases should be kept in mind:

1. The charged mode Λ's have a 5 mm. cut-off.

2. The distribution of neutral decays should be distorted by the expected dependence of conversion probability on the position in the chamber and the momentum of the Λ.

3. Measuring error should tend to increase the apparent decay

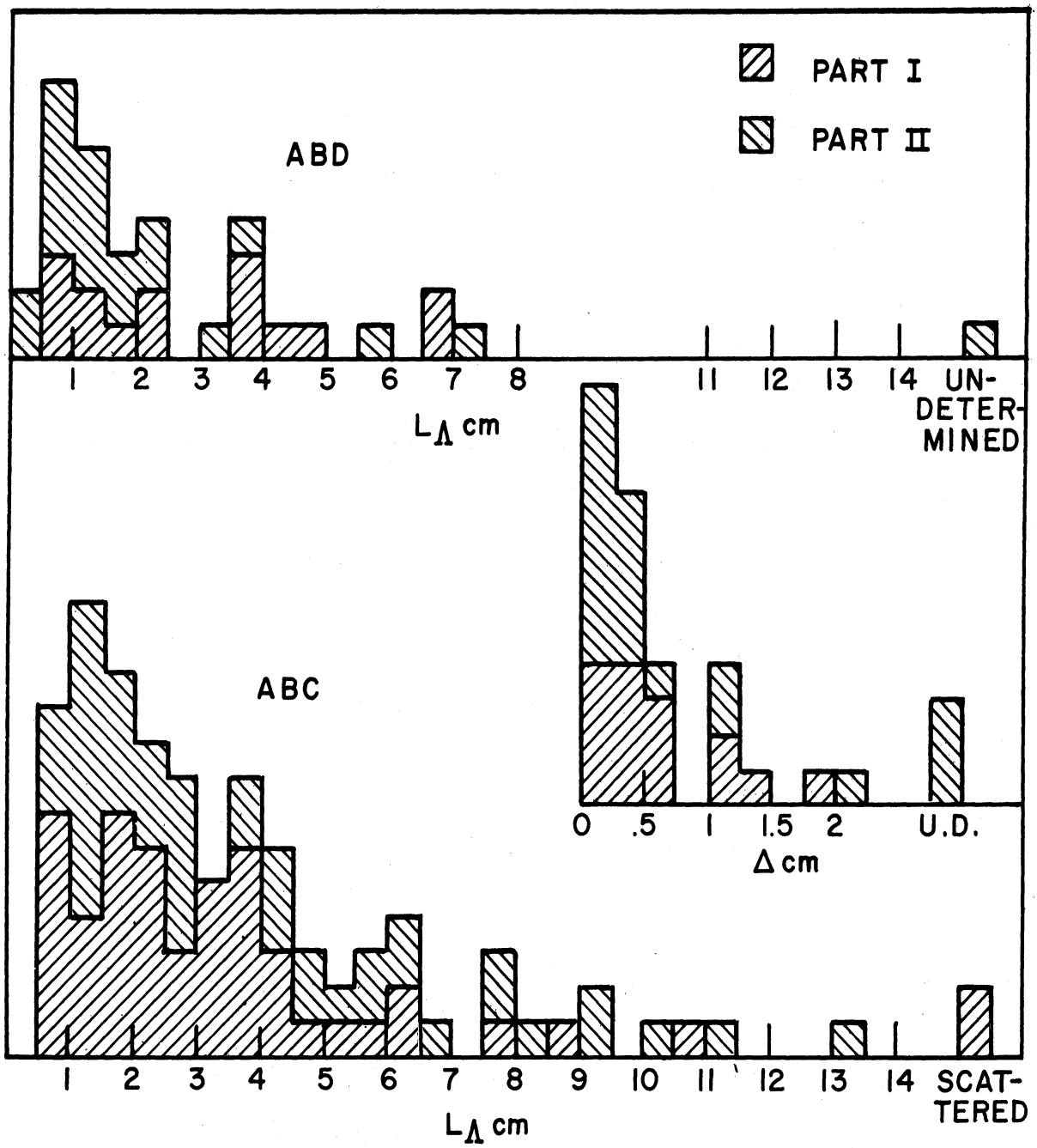

Fig. 12. Decay Length Distributions for ABC and ABD with Δ Distribution for ABD.

lengths of the neutral decays. An estimate of the size of the errors expected in determining the origin of the two associated gamma rays can be got from the distribution of the distance of closest approach, Δ, for the extensions of the measured paths of two associated gammas, as seen in Fig.12.

As a parameter for comparing the two distributions let us choose the average decay length, $\bar{L}_\Lambda$, for each distribution. For the 32 neutral events (ABD) for which L_Λ could be determined we find

$$\bar{L}_{\Lambda \text{ neutral}} = 2.39 \pm .35 \text{ cm.}$$

Instead of comparing this directly with the average of the ABC events let us rather consider an adjusted average defined in the following manner:

$$\bar{L}_{\Lambda \text{ charged, adjusted}} = \frac{L' + .21x.25}{1.21}$$

where L' is a weighted average of the ABC Λ's run in the Monte Carlo calculations described on page 28 and is given by

$$L' = \sum_{i=1}^{92} w_i L_{\Lambda i} \Big/ \sum_{i=1}^{92} w_i$$

where w_i is an integer from 0 to 5 and is the number of times out of five passes the event was found by the Monte Carlo calculation to have both gammas convert. The term .21x.25 is the correction for the 21% of the ABC type Λ's that would be expected to decay less than 5 mm. from the origin (see page 27). The factor 1.21 in the denominator is the proper normalization factor.

One finds

$$\bar{L}_{\Lambda \text{ charged, adjusted}} = 3.09 \pm .25 \text{ cm.}$$

This result neglects effects due to measuring errors. The chance that these two measurements of what we presume is the same quantity differ by .70 cm or more is about one in ten. We can therefore state that the two average decay lengths are not inconsistent with a common lifetime for the events satisfying C and those satisfying D.

It is reassuring to note that the average potential path for the ABC Λ's is $13.02 \pm .52$ cm., and that if the neutral decays were random in the chamber we would expect the average "decay length" to be more like half the average potential path, rather than the much smaller number we have stated above.

C. The mass of the π° from the Λ.

As shown in Appendix C it is possible to measure the mass of the π° from the Λ decay by looking at the distribution of the opening angle, χ, between the two gamma rays from the π° and the distribution of the momentum, P_Λ, of the Λ population as got from the charged mode events.

We see in fact from equations C 1.9 and C 1.11 that

$$m_{\pi^0} = m_\Lambda \left(1 + \frac{p^{*2}}{m_{\pi^0}^2} \right)^{1/2} - \left(m_\Lambda^2 \frac{p^{*2}}{m_{\pi^0}^2} + m_N^2 \right)^{1/2}$$

where $$\frac{p^{*2}}{m_{\pi^0}^2} = \frac{3/2 \, \overline{\cot^2 \chi/2} - \overline{P_\Lambda^2}/m_\Lambda^2}{1 + 4/3 \, \overline{P_\Lambda^2}/m_\Lambda^2}$$

where P* is the momentum of the π° in the CM of the Λ and is, of course, a function of the π° mass.

As an unbiased sample we choose the events used in the Monte Carlo calculation. The momentum distribution of this sample can be seen in Fig. 13.

We find

$$\overline{P_\Lambda^2} = (3.23 \pm .23) \times 10^5 \ (\text{Mev/c})^2$$

The sample of π°'s we choose to be 30 of the 35 ABD events for which both gamma rays produced well-defined and measureable electron pairs. The distribution for χ for these events is given in Fig. 13. We find

$$\overline{\cot^2(\chi/2)} = .97 \pm .14$$

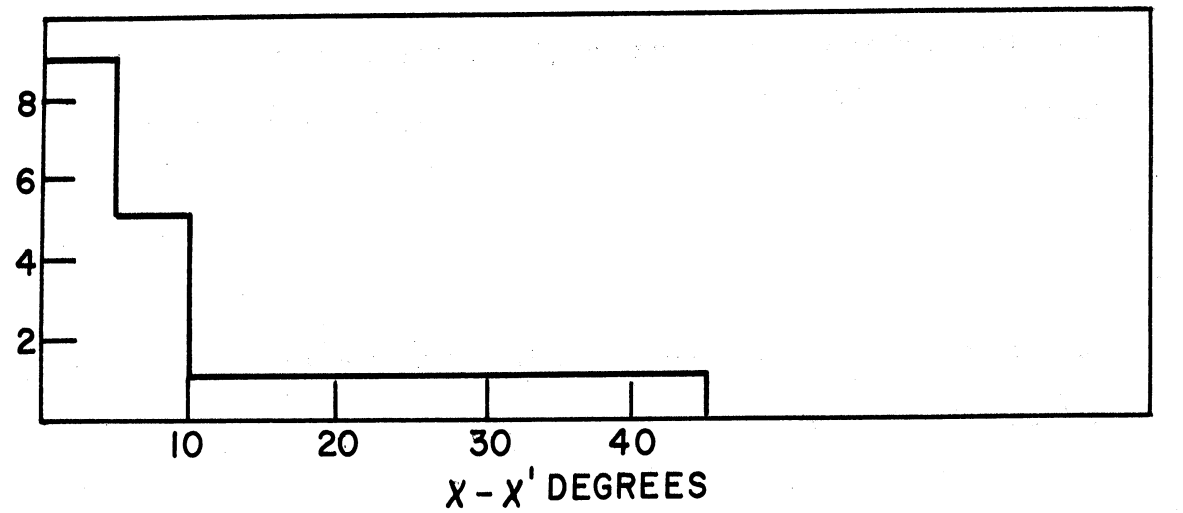

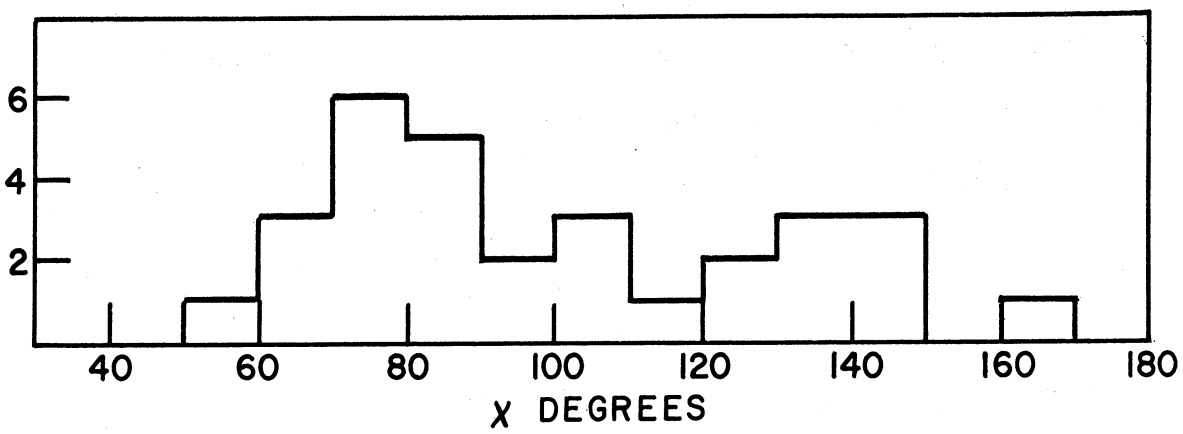

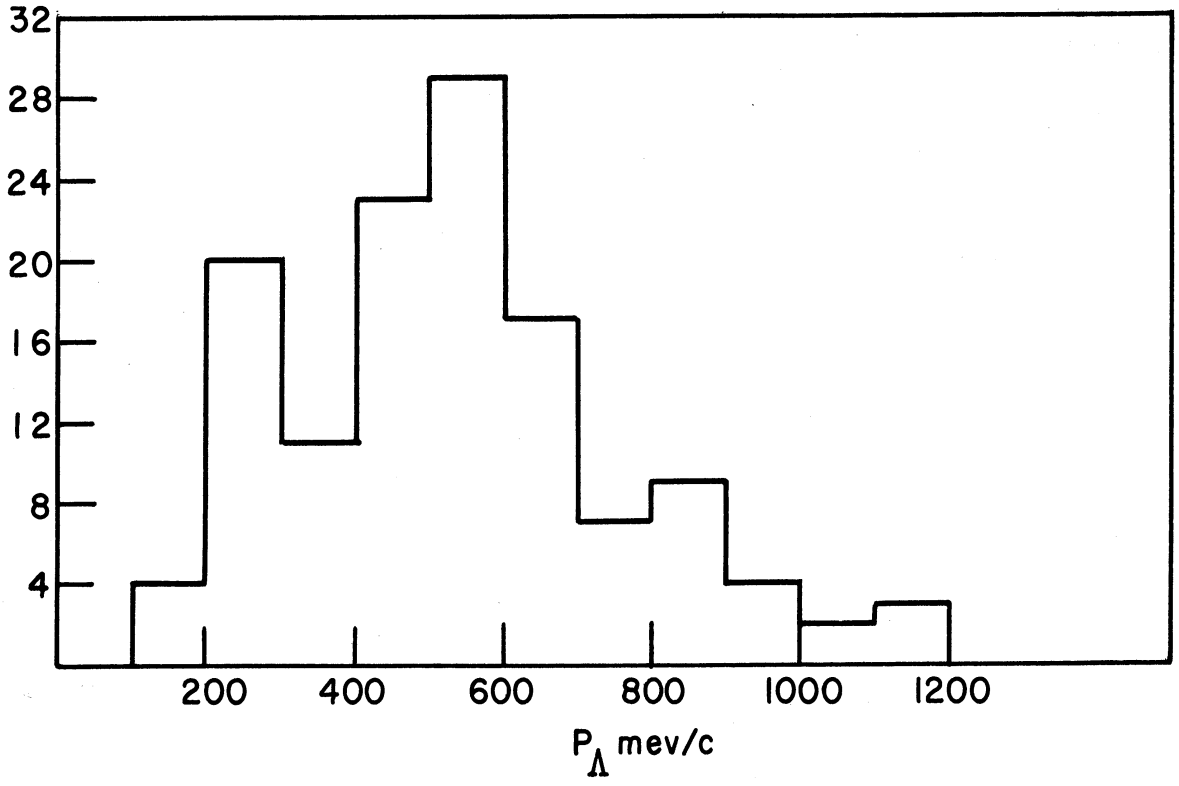

Fig. 13. Momentum of Monte Carlo Λ's, χ Distribution, and Distribution of Difference in χ for Two Measurement.

This number must be corrected for skewness due to the error in determining χ as explained in Appendix C2. Using an average square error (in radians)

$$\overline{\epsilon^2} = .038$$

as got from 21 pairs of gamma pairs that were measured twice in part I (see Fig.13), we find

$$\cot^2\chi/2_{\text{corrected}} = .89 \pm .13$$

where $\cot^4\chi/2$ was taken as 1.51 as calculated from the 30 ABD events and was not corrected for skewness.

Inserting these numbers into the equations on the preceding page we find

$$M_{\pi^\circ} = 126 \pm 6 \text{ Mev}$$

where the error is one standard deviation.

This number should be taken as evidence that the neutral mode of the Λ decay is indeed

$$\Lambda \rightarrow \pi^\circ + \text{neutron}.$$

Appendix A. The Pionic decay of the Λ, V-A theory, and the $\Delta I=1/2$ rule

A1. Channels for the decay

If the spin of the Λ is 1/2 and the final states are not required to be eigenstates of the parity operator, one can describe the final states of the Λ by four complex numbers

$$\begin{aligned} S_1 &= |S_1| e^{i\delta_1} \\ S_3 &= |S_3| e^{i\delta_3} \\ P_1 &= |P_1| e^{i\delta_{11}} \\ P_3 &= |P_3| e^{i\delta_{31}} \end{aligned} \qquad \text{A1.1}$$

where S and P correspond respectively to L = 0 and L = 1, where L is the orbital angular momentum of the pion-nucleon system, and where the subscripts 1 and 3 correspond respectively to the two isotopic spin states, I = 1/2 and I = 3/2, possible for a pion-nucleon system in general.

If the decay is invariant under time reversal, it can be shown (18) that the relative phases, δ , are just those expected from π-N scattering at the energy in the CM given by the Q value (about 40 Mev).

The experimental values for these phase shifts are (19)

$$\begin{aligned} \delta_1 &= +\ 8^\circ \\ \delta_3 &= -\ 4^\circ \\ \delta_{11} &= 0 \\ \delta_{31} &= 0 \end{aligned} \qquad \text{A1.2}$$

Thus the amplitudes are real to within one percent. We shall

neglect the imaginary parts.

A2. Charge distribution

With the help of the Clebsch-Gordan coefficients we can relate the two charge states ($\pi^- + p^+$ denote "-" and $\pi^\circ + n^\circ$ denote "0") to the isotopic spin states.

A2.1 $$\begin{pmatrix} S_0 \\ P_0 \end{pmatrix} = -\sqrt{\frac{1}{3}}\begin{pmatrix} S_1 \\ P_1 \end{pmatrix} + \sqrt{\frac{2}{3}}\begin{pmatrix} S_3 \\ P_3 \end{pmatrix}$$

and

A2.2 $$\begin{pmatrix} S_- \\ P_- \end{pmatrix} = \sqrt{\frac{2}{3}}\begin{pmatrix} S_1 \\ P_1 \end{pmatrix} + \sqrt{\frac{1}{3}}\begin{pmatrix} S_3 \\ P_3 \end{pmatrix}$$

Then the ratio of neutral to charged mode is given by

A2.3 $$R = \frac{S_0^2 + P_0^2}{S_-^2 + P_-^2}$$

or

A2.4 $$R = \frac{(1+z^2) - 2\sqrt{2}(x+z^2y) + 2(x^2+y^2z^2)}{2(1+z^2) + 2\sqrt{2}(x+z^2y) + (x^2+y^2z^2)}$$

where

$$x = \frac{S_3}{S_1}, \quad y = \frac{P_3}{P_1} \quad \text{and} \quad z = \frac{P_1}{S_1}$$

A.3 The angular distributions

Assuming parity is conserved in the Λ production process the Λ can have no component of polarization on the production plane. Let us define "up" as the direction of the production plane normal (the vector product of a unit vector in the beam direction with a unit vector in the Λ direction).

The wave function for the Λ with spin up may be written

A3.1 $$\psi_{up} = S\alpha Y_0^0 + P\left(\sqrt{\tfrac{1}{3}}\alpha Y_1^0 - \sqrt{\tfrac{1}{3}}\beta Y_1^1\right)$$

and with spin "down"

A3.2 $$\psi_{down} = S\beta Y_0^0 + P\left(-\sqrt{\tfrac{1}{3}}\beta Y_1^0 + \sqrt{\tfrac{2}{3}}\alpha Y_1^{-1}\right)$$

where α and β are the spin functions for the nuclear spin up and down, respectively, S and P are either S_0, P_0 or S_-, P_-, and the Y's are the first four spherical harmonics:

$$Y_0^0 = \frac{1}{(4\pi)^{1/2}}$$

A3.3 $$Y_1^0 = \left(\frac{3}{4\pi}\right)^{1/2}\cos\xi^*$$

$$Y_1^{\pm 1} = \left(\frac{3}{8\pi}\right)^{1/2}\sin\xi^* e^{\pm i\eta^*}$$

where ξ^* and η^* are polar and azimuthal angles of the decay pion in the CM system of the Λ as shown in Fig. 14.

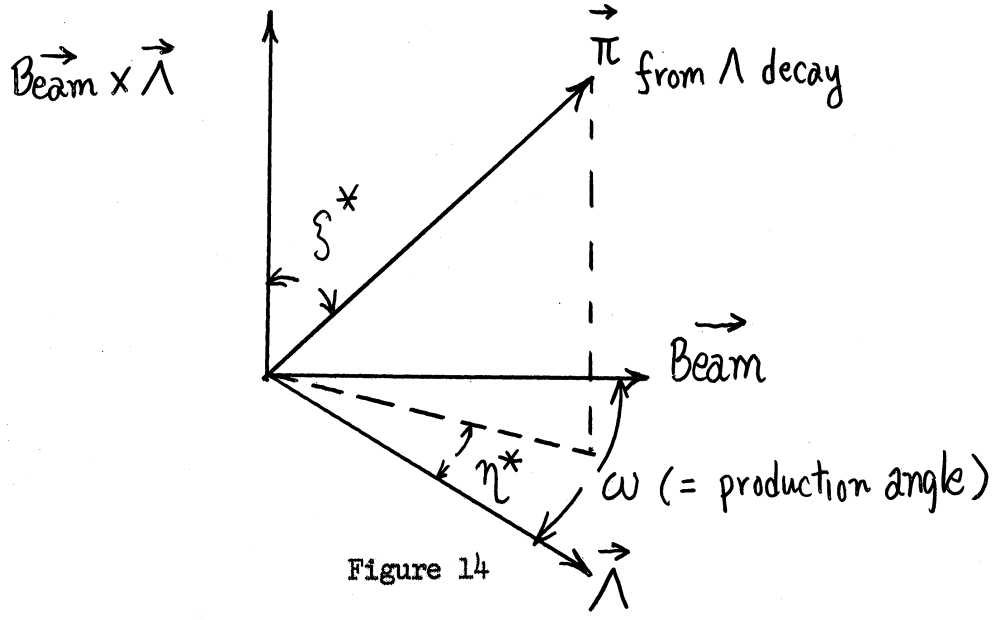

Figure 14

The angular distribution of the decay pion from Λ's with spin up will be

A3.4 $$\psi^*_{up}\,\psi_{up} = \frac{S^2+P^2}{4\pi}\left(1+\alpha\cos\xi^*\right)$$

or

A3.5 $$\left(\frac{dI}{d\Omega}\right)_{\Lambda\ spin up} = \frac{1+\alpha\cos\xi^*}{4\pi}$$

where we have defined

A3.6 $$\alpha = \frac{2Re\ S^*P}{S^2+P^2}$$

Likewise

A3.7 $$\left(\frac{dI}{d\Omega}\right)_{\Lambda\ spin\ down} = \frac{1-\alpha\cos\xi^*}{4\pi}$$

Now if we define the fraction of Λ's with spin up to be F_{up} and the fraction down to be

$$F_{down} = 1 - F_{up}$$

averaged over all production angles (ω, see Fig. 14), then the average polarization will be

A3.8 $$\bar{P} = F_{up} - F_{down}$$

and therefore for the total sample we will have

A3.9 $$\frac{dI}{d\Omega} = \frac{1}{4\pi}\left(1+\alpha\bar{P}\cos\xi^*\right)$$

For the charge mode we find

A3.10 $$\alpha_- = 2Z\frac{2+\sqrt{2}(X+y)+Xy}{2(1+Z^2)+2\sqrt{2}(X+Z^2y)+(X^2+Z^2y^2)}$$

and for the neutral mode

A3.11 $$\alpha_0 = 2z\,\frac{1-\sqrt{2}(x+y)+2xy}{1+z^2-2\sqrt{2}(x+z^2y)+2(x^2+y^2z^2)}$$

where x, y, z are as defined above.

A4. Predictions of the $|\vec{\Delta I}| = 1/2$ Rule

Gell-Mann and Pais (20) have suggested that there may be a selection rule that the total isotopic spin changes by 1/2 in the decay of a strange particle. For the case of the lambda this means x = y = 0.

Then

$$R = 1/2$$

A4.1 and

$$\alpha_0 = \alpha_- = \frac{2z}{1+z^2}$$

It is important to point out, however, that R = 1/2 and $\alpha_0/\alpha_- = 1$ are not sufficient conditions that the $|\vec{\Delta I}| = 1/2$ rule hold.

Let us consider the quantities

A4.2 $$R = \frac{(1+z^2)-2\sqrt{2}(x+z^2y)+2(x^2+z^2y^2)}{2(1+z^2)+2\sqrt{2}(x+z^2y)+(x^2+y^2z^2)}$$

and

A4.3 $$R\left(\frac{\alpha_0}{\alpha_-}\right) \equiv r = \frac{1-\sqrt{2}\,x-\sqrt{2}\,y+2xy}{2+\sqrt{2}\,x+\sqrt{2}\,y+xy}$$

Equation A4.2 can be written

A4.4 $$\left[x+\sqrt{2}\left(\frac{R+1}{R-2}\right)\right]^2+z^2\left[y+\sqrt{2}\left(\frac{R+1}{R-2}\right)\right]^2=\frac{9R(1+z^2)}{(R-2)^2}$$

which one can see is a two-parameter family of ellipses in the x-y plane. If R = 1/2 and $z^2 = 1$ (parity non-conservation is maximum) we have

A4.5 $$(x-\sqrt{2})^2 + (y-\sqrt{2})^2 = 4$$

Equation A4.3 can be written

A4.6 $$\left[x+y+2\sqrt{2}\left(\frac{r+1}{r-2}\right)\right]^2 - (x-y)^2 = \frac{36r}{(r-2)^2}$$

which is a one-parameter family of hyperbolae on the x-y plane. If r = 1/2

A4.7 $$(x+y-2\sqrt{2})^2 - (x-y)^2 = 8$$

From Fig. 15 we see that, if $\alpha_+/\alpha_- = 1$ and R = 1/2, we have restricted ourselves to the region x = y = 0 ($|\vec{\Delta I}| = 1/2$) or $x = y = 2\sqrt{2}$. If z^2 differs from 1, the circle will become an ellipse with axes parallel to the x-y axes and still passing through the points x = y = 0 and $x = y = 2\sqrt{2}$.

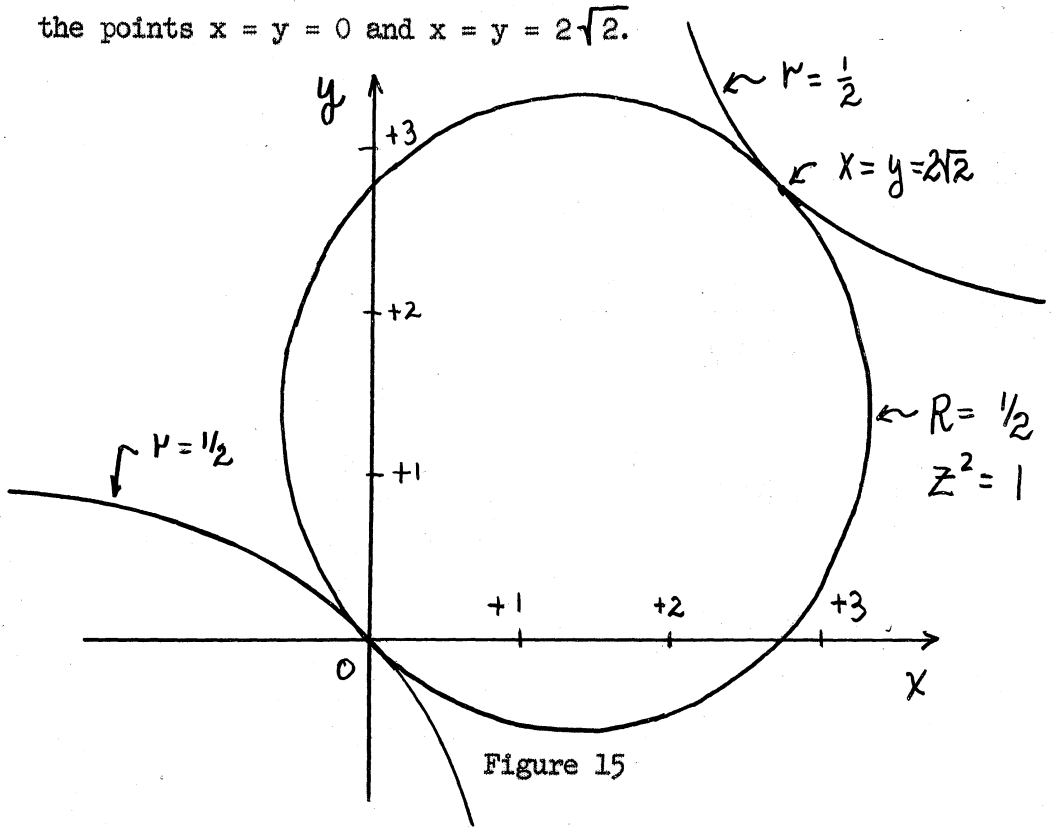

Figure 15

A5. Predictions of the V-A Theory

Okubo, Marshak, and Sudarshan (21) have stated that extension of the V-A theory to the Λ decay gives rather uniquely for the weak interaction producing the decay

A5.1 $$H_W = G\bar{\psi}_p \gamma^\lambda (1+\gamma_5)\psi_\Lambda \cdot \bar{\psi}_n \gamma_\lambda (1+\gamma_5)\psi_p + H.C.$$

where G is the universal weak-coupling constant, ψ_p, ψ_n, ψ_Λ are the wave functions for the proton, neutron, and Λ, and the γ's are the well-known Dirac γ's.

Using the Born approximation the above authors show that their postulated H_W (A5.1) gives

A5.2 $$x = y = 2\sqrt{2}$$

Thus we see from Fig. 15 that V-A theory in lowest approximations also predicts R = 1/2 and $\alpha_0/\alpha_- = 1$.

However the above authors also show that higher approximations lead to slightly different predictions from those of the Born approximation, and, although present experimental results are too imprecise to decide between the V-A theory and the $|\vec{\Delta I}| = 1/2$ rule, such a decision in principle could be made on the basis of precisely determined values for R and α_0/α_-.

It is amusing to note then that there is at present no good reason for preferring either one of the two intersection points of the curves in Fig. 15 as indicating roughly the relative abundances of $|\vec{I}| = 3/2$ to $|\vec{I}| = 1/2$ participating in the Λ decay.

A6. Phase space correction

Because of the difference in the masses of the decay products for the two pionic decay modes of the Λ one expects that there should be slightly different amounts of phase space available to the two modes. Indeed this is so; assuming for instance that the $\left|\vec{\Delta I}\right| = 1/2$ rule is correct we find that

$$R = .3390 \text{ instead of } 1/3$$

Appendix B. The Determination of the Asymmetry Parameter of the Neutral Mode

B0. As shown in appendix A the angular distribution of the π° in the Λ CM is given by

B0.1 $$\frac{dI}{d\Omega^*} = \frac{1}{4\pi}\left(1 + \alpha_0 \bar{P} \cos\xi^*\right)$$

where $$d\Omega^* = d\eta^*\, d\cos\xi^*$$

We shall approach the problem of determining $\alpha\bar{P}$ first by looking at the distribution of the gammas and second by looking at the distribution of the bisector of the angle between the gammas. Unless otherwise indicated the asterisk will denote the Λ CM.

B1. Angular distribution of the gammas

In the following we shall show that the form of the distribution for gammas from the Λ is the same as that for the π°, with the asymmetric term being multiplied by a "washout" factor which we shall calculate.

Let us first consider the general case of a distribution on the unit sphere given by $F_\circ(\xi)$ where ξ is the polar angle and there is no dependence on the azimuthal angle η. Now let us introduce a disordering process $D(\phi)$, which is the probability that a point on the unit sphere will be moved to a point within an area $\sin\xi' d\xi' d\eta'$, a distance ϕ away, i.e. a point at ξ, η will be moved to ξ', η' where

B1.1 $$\cos\phi = \cos\xi\cos\xi' + \sin\xi\sin\xi'\cos(\eta - \eta')$$

$D(\phi)$ is independent of ξ and η.

Then the disordered distribution can be written

$$\text{B1.2} \quad F(\xi,\eta) = \int_0^{2\pi}\int_0^{\pi} D(\phi)\, F_0(\xi') \sin\xi' d\xi' d\eta'$$

where $D(\phi)$ has the condition that

$$\text{B1.3} \quad \int_0^{2\pi}\int_0^{\pi} D(\phi) \sin\xi' d\xi' d\eta' = 1$$

Expand $D(\phi)$ in terms of the Legendre polynomials

$$\text{B1.4} \quad D(\phi) = \sum_{n=0}^{\infty} b_n P_n(\cos\phi)$$

and use the addition theorem

$$\text{B1.5} \quad P_n(\cos\phi) = P_n(\cos\xi) P_n(\cos\xi') + 2\sum_{m=1}^{n} \frac{(n-m)!}{(n+m)!} P_n^m(\cos\xi) P_n^m(\cos\xi') \cos m(\eta-\eta')$$

Expand $F_0(\xi)$ in the Legendre polynomials

$$\text{B1.6} \quad F_0(\xi) = \sum_{n=0}^{\infty} a_n P_n(\cos\xi)$$

Then using the orthogonality relations we get

$$\text{B1.7} \quad F(\xi) = 2\pi \sum_{n=0}^{\infty} \frac{a_n b_n}{2n+1} P_n(\cos\xi)$$

Now we must find $D(\phi)$ for the case of gammas from the Λ. In the CM of the Λ the π° has a unique velocity, so $D(\phi)$ is just the probability that a gamma will come off at an angle ϕ from the line of flight of the π°. Let us denote the velocity of the π° in units of the speed of light as β.

Let P be the momentum of the gamma and ϕ be the angle with respect to the line of flight of the π° in the CM of the π°. Let

P* and ϕ^* be the corresponding quantities in the CM of the Λ.

Then if $\gamma = (1 - \beta^2)^{-1/2}$ we have from the Lorentz transformation

B1.8
$$\begin{pmatrix} P^* \cos\phi^* \\ P^* \sin\phi^* \\ 0 \\ iP^* \end{pmatrix} = \begin{pmatrix} \gamma & 0 & 0 & i\beta\gamma \\ 0 & 1 & 0 & 0 \\ 0 & 0 & 1 & 0 \\ -i\beta\gamma & 0 & 0 & \gamma \end{pmatrix} \begin{pmatrix} P\cos\phi \\ P\sin\phi \\ 0 \\ iP \end{pmatrix}$$

Then we find

B1.9
$$\cos\phi = \frac{\cos\phi^* - \beta}{1 - \beta\cos\phi^*}$$

or

B1.10
$$\sin\phi\, d\phi = \frac{1-\beta^2}{(1-\beta\cos\phi^*)^2} \sin\phi^* d\phi^*$$

Now the gamma distribution is isotropic in the π° CM if the π° has no spin, i.e.

B1.11
$$\frac{dI_\gamma}{d\Omega} = \frac{1}{4\pi}$$

Therefore

B1.12
$$\frac{dI_\gamma}{d\Omega} = \frac{1}{4\pi} \frac{1-\beta^2}{(1-\beta\cos\phi^*)^2} \equiv D(\phi^*)$$

Now we expand $D(\phi^*)$ in the Legendre polynomials with interest only in the first two terms

B1.13
$$D(\phi^*) = \frac{1}{4\pi}\left(1 + 3 w_\gamma \cos\phi^* + \cdots\right)$$

Inserting this expansion into equation B1.7 we find

B1.14
$$\frac{dI_\gamma}{d\Omega} = \frac{1}{4\pi}\left[1 + w_\gamma \alpha_0 \bar{P} \cos\xi_\gamma^*\right]$$

where the "washout" factor W_γ is given by

B1.15 $$W_\gamma = \frac{1-\beta^2}{2\beta^2}\left(\ln\left(\frac{1-\beta}{1+\beta}\right) + \frac{2\beta}{1-\beta^2}\right)$$

For $\beta = 0.61$, we find $W_\gamma = 0.43$.

B2. Angular distribution of the bisector of the angle between the gammas

Analogously to B1 we find for the distribution of the bisector of the angle between the two gammas, $\vec{B}$, to be

B2.1 $$D(\phi) = \frac{1}{2\pi}\frac{(1-\beta^2)\cos\phi}{\sin\phi\,(1-\beta^2\cos^2\phi)^{3/2}} \quad \text{for } \phi \leq \frac{\pi}{2}$$

$$D(\phi) = 0 \quad \text{for } \phi > \pi/2$$

where ϕ is defined by Fig. 16.

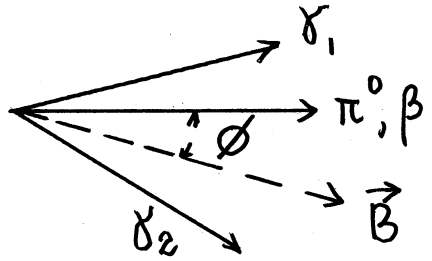

Figure 16

Expanding $D(\phi)$ in Legendre polynomials

B2.2 $$D(\phi) = \frac{1}{4\pi}\left[1 + 3\,w_B\cos\phi + \cdots\right]$$

where

B2.3 $$w_B = (1-\beta^2)\int_0^1 \frac{x^2\,dx}{(1-x^2)^{1/2}(1-\beta^2x^2)^{3/2}}$$

Then

B2.4 $$\frac{dI}{d\Omega_B} = \frac{1}{4\pi}\left(1 + W_B \alpha_0 \bar{P} \cos \xi_B^*\right)$$

For $\beta = 0.61$, $W_B = 0.82$.

B3. We can now decide which of these two approaches yield the most information. Let us look for example at the fractional error in determining the average value of $\cos \xi^*$. One can show

B3.1 $$\frac{\overline{\Delta \cos \xi^*}}{\overline{\cos \xi^*}} = \sqrt{\frac{3 - A^2}{A^2 N}}$$

where $A = W\alpha\bar{P}$ and N is the number of events. Taking as a reasonable value for $\alpha\bar{P}$ as 1/2 one can see the bisector method is more accurate by a factor of about $\sqrt{2}$. It is clear that the latter method should provide more information since it takes into account the correlations of the gammas in pairs, whereas the former method treats all gammas independently.

B4. The above distributions are given for the Λ CM and the distributions in the LAB are in general more complicated since the Lorentz transformation is not independent of ξ and η. Moreover, since in the xenon chamber one cannot infer the momentum of the Λ from the gamma rays alone, because their energies cannot be determined, one cannot transform into the Λ CM.

The projections of four-vectors onto the plane perpendicular to the line-of-flight are however invarient under Lorentz transformations of the vectors in the direction of the line-of-flight. Let us choose a new coordinate system so that the new azimuthal angle, ψ, lies in this plane as shown in Fig. 17

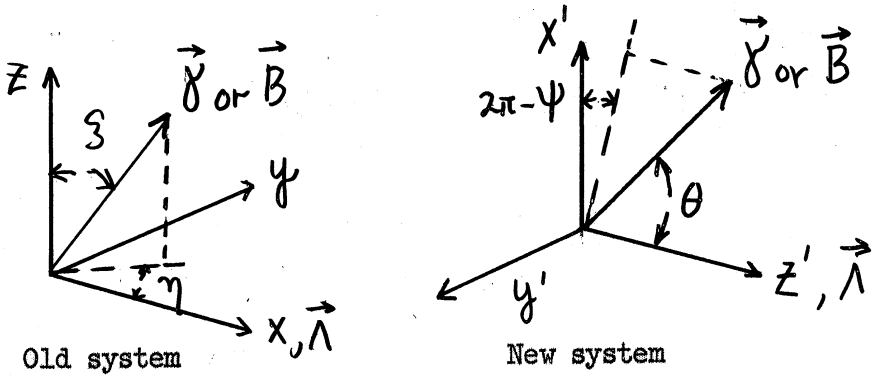

Figure 17

Then still in the CM we can write

B4.1 $$\frac{dI}{d\psi_\gamma^*} = \frac{1}{2\pi}\left(1 + \frac{\pi}{4} W_\gamma \alpha_0 \bar{P} \cos\psi_\gamma^*\right)$$

and

B4.2 $$\frac{dI}{d\psi_B^*} = \frac{1}{2\pi}\left(1 + \frac{\pi}{4} W_B \alpha_0 \bar{P} \cos\psi_B^*\right)$$

In the first case since the gammas are four vectors we can write also for the LAB

B4.3 $$\frac{dI}{d\psi_\gamma} = \frac{1}{2\pi}\left(1 + \frac{\pi}{4} W_\gamma \alpha_0 \bar{P} \cos\psi_\gamma\right)$$

For the bisectors no such simple relation exists. Indeed if λ^*, μ^*, ν^* are the direction cosines of a gamma in the CM on the x', y', and z' axes, respectively, then

B4.4 $$\cos\psi_B^* = \frac{\lambda_1^* + \lambda_2^*}{\sqrt{(\lambda_1^* + \lambda_2^*)^2 + (\mu_1^* + \mu_2)^2}}$$

The direction cosines transform as

$$\lambda^* = (\lambda/\gamma)/(1-\beta\nu)$$

B4.5 $$\mu^* = (\mu/\gamma)/(1-\beta\nu)$$

$$\nu^* = (\nu-\beta)/(1-\beta\nu)$$

B5. Error in azimuthal distribution

Suppose we wish to determine $A = \frac{\pi}{4} W(\alpha) \bar{P}$ from N events say in formula B4.3 above, then the "S function" (17) is

B5.1 $$S(A) = \Delta A \sum_{i=1}^{N} \frac{\cos\psi_i}{1 + A\cos\psi_i}$$

where

B5.2 $$\Delta A = \frac{1}{\sqrt{N}} \left[\frac{1}{2\pi} \int_0^{2\pi} \frac{\cos^2\psi \, d\psi}{1 + A\cos\psi} \right]^{-1/2}$$

$$= \frac{1}{\sqrt{N}} \left[\frac{1-\sqrt{1-A^2}}{A^2\sqrt{1-A^2}} \right]^{-1/2} \text{ for } A<1$$

Appendix C. The Mass of the π° from the Decay of the Λ

C1. Derivation

By application of the Lorentz transformation to a π° whose momentum and mass are designated by P_{π° and M_{π°, respectively, one can show that

C1.1
$$\cot \frac{\chi}{2} = \frac{P_{\pi^\circ}}{M_{\pi^\circ}} \sin \alpha$$

where χ is the angle between the gammas from the decay of the π° in LAB and α is the π° CM decay angle, as shown in Fig. 18.

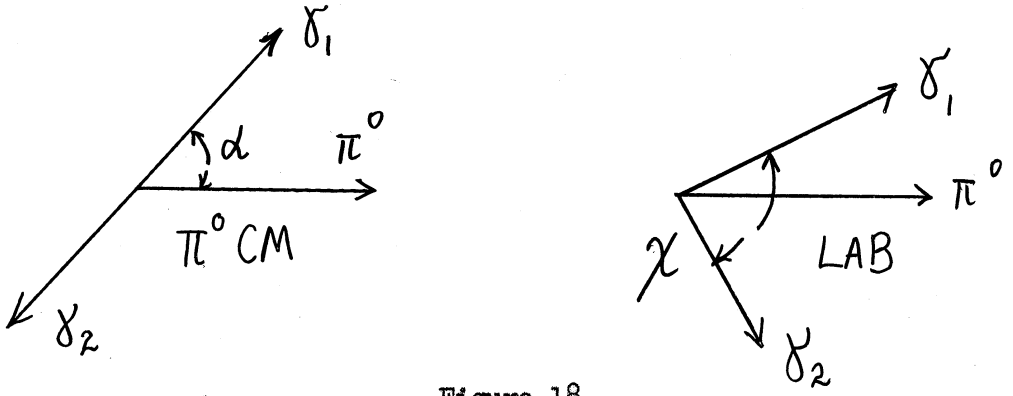

Figure 18

Application of the Lorentz transformation to the Λ decay gives

C1.2
$$P_{\pi^\circ} \cos \theta_{\pi^\circ} = \gamma_\Lambda \left(P^* \cos \theta^*_{\pi^\circ} + \beta_\Lambda E^* \right)$$
$$P_{\pi^\circ} \sin \theta_{\pi^\circ} = P^* \sin \theta^*_{\pi^\circ}$$

where β is the velocity in units of the speed of light of the Λ in the LAB and $\gamma_\Lambda = (1 - \beta_\Lambda^2)^{-1/2}$. θ_{π° and $\theta^*_{\pi^\circ}$ are the angles the π° makes with the Λ line of flight in LAB and Λ CM, respectively, as shown in Fig. 19.

Figure 19

Then

C1.3 $$P_{\pi^0}^2 = \gamma_\Lambda^2 \left[P^{*2} + 2\beta_\Lambda P^* E^* \cos\theta^*_{\pi^0} - \beta_\Lambda^2 P^{*2} \sin^2\theta^*_{\pi^0} + \beta_\Lambda^2 E^{*2} \right]$$

One can easily show that equation B0.1 can be written in the coordinate system in which θ^* is the polar angle and ψ^* is the azimuthal angle as

C1.4 $$\frac{dI}{d\cos\theta^*_{\pi^0} d\psi^*} = \frac{1}{4\pi}\left[1 + \alpha \bar{P} \cos\psi^* \sin\theta^*_{\pi^0} \right]$$

Integrating over ψ^* we get

C1.5 $$\frac{dI}{d\cos\theta^*_{\pi^0}} = \frac{1}{2}$$

Since the π° is presumed spinless we have also

C1.6 $$\frac{dI}{d\cos\alpha} = \frac{1}{2}$$

Eliminating P_{π° from equations C1.1 and C1.3 and averaging over α, θ^* and β_Λ we get

C1.7 $$3/2\ \overline{\cot^2\frac{\chi}{2}} = \frac{P^{*2}}{M_{\pi^0}^2}\left[\frac{1}{3}\overline{\beta_\Lambda^2\gamma_\Lambda^2} + \overline{\gamma_\Lambda^2} \right] + \overline{\beta_\Lambda^2\gamma_\Lambda^2}$$

Noting that

C1.8 $$P_\Lambda = \beta_\Lambda \gamma_\Lambda M_\Lambda \qquad \text{and} \qquad E_\Lambda = \gamma_\Lambda M_\Lambda$$

where P_Λ, E_Λ and M_Λ are the momentum, energy, and mass, respectively, of the Λ; we find then

C1.9 $$\frac{p^{*2}}{M_{\pi^0}^2} = \frac{3/2\ \overline{\cot^2 \frac{\chi}{2}} - \overline{P_\Lambda^2}/M_\Lambda^2}{1 + 4/3\ \overline{P_\Lambda^2}/M_\Lambda^2}$$

Finally using the fact that

C1.10 $$M_\Lambda = (p^{*2} + M_{\pi^0}^2)^{1/2} + (p^{*2} + M_N^2)^{1/2}$$

(Note that P* is a function of M_{π^0}.)

we can express the mass of the π° in terms of measurable quantities

C1.11 $$M_{\pi^0} = M_\Lambda \left(1 + \frac{p^{*2}}{M_{\pi^0}^2}\right)^{1/2} - \left(M_\Lambda^2 \frac{p^{*2}}{M_{\pi^0}^2} + M_N^2\right)^{1/2}$$

M_N is the neutron mass.

C2. Skewness correction for $\cot^2 \chi/2$

In calculating the average value of $\cot^2 \chi/2$ a correction must be made for the error in measuring χ. Let us suppose the error in measuring χ is ϵ, then

C2.1 $$\chi_{\text{measured}} = \chi + \epsilon$$

To second order in ϵ

C2.2 $$\cot^2\left(\frac{\chi+\epsilon}{2}\right) = \cot^2\frac{\chi}{2} - \epsilon \cot\frac{\chi}{2} \csc^2\frac{\chi}{2} + \epsilon^2\left(\frac{1}{4} + \cot^2\frac{\chi}{2} + 3/4 \cot^4\frac{\chi}{2}\right)$$

Averaging over all measurements we expect

C2.3 $$\overline{\epsilon} = 0$$

and

C2.4 $$\overline{\cot^2 \frac{\chi}{2}} \simeq \frac{\overline{\cot^2 \frac{\chi+\epsilon}{2}} - \overline{\epsilon^2}\left(\frac{1}{4} + 3/4\ \overline{\cot^4 \frac{\chi}{2}}\right)}{1 + \overline{\epsilon^2}}$$

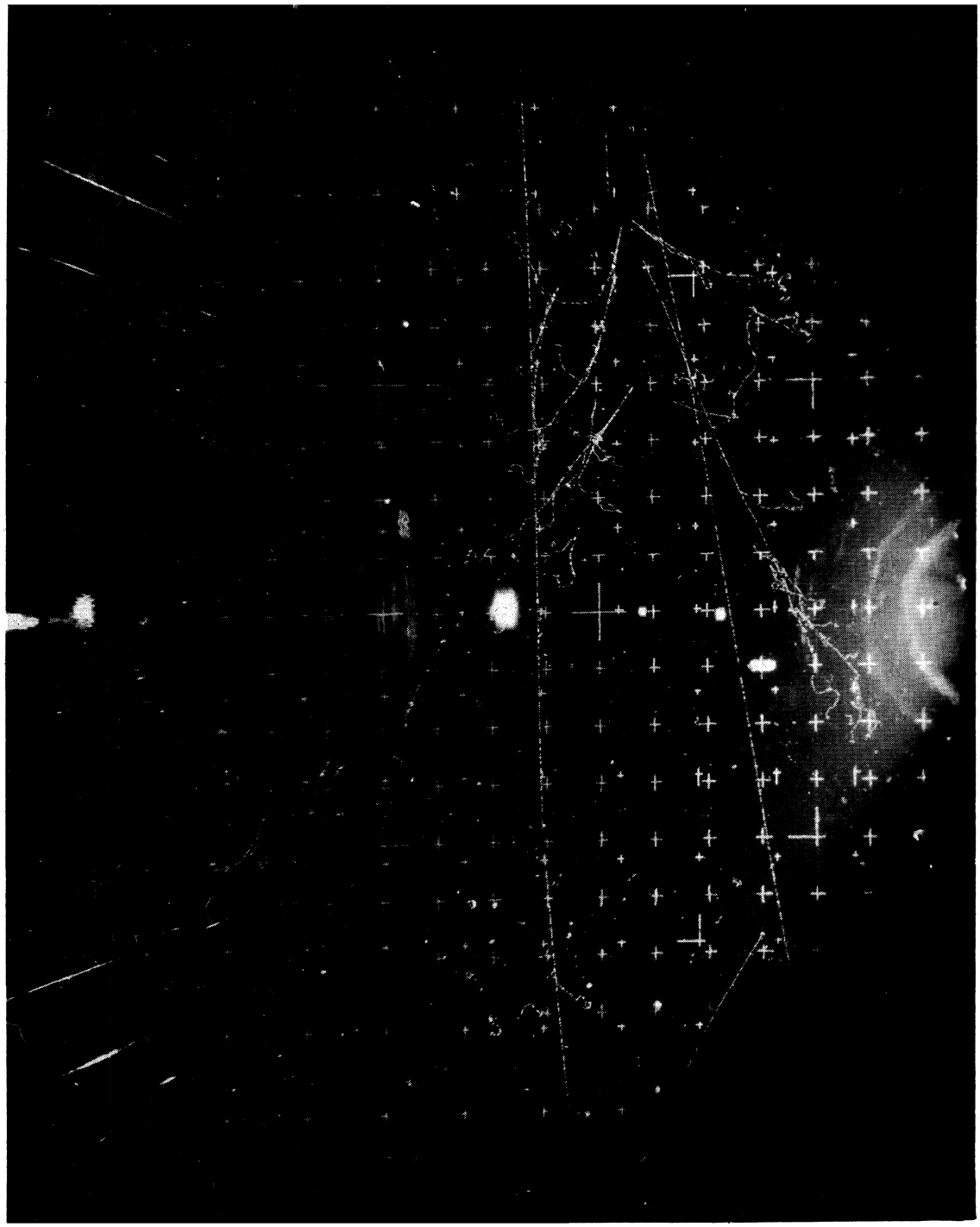

Fig. 20. Photograph of "Complete" Neutral Decay.

Appendix D. Search for "Complete" Neutral Decay of the Λ

No clear cut cases of interactions in the xenon chamber of the neutron from the decay of the Λ were found in pictures containing a charged K_1° mode and two associated gammas (ABD events), although each picture was carefully scanned. However one event was discovered, more or less by accident, of the AD type for which the neutron apparently interacted and the K_1° decayed neutrally. This was frame number 115,441, shown in Fig. 20. The interpretation of this event is shown in Fig. 21.

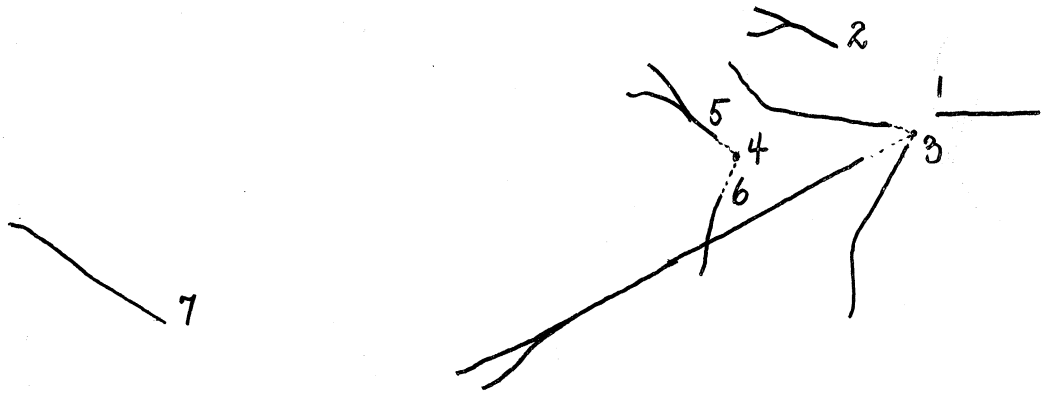

Figure 21

where the stations denote the following occurrences

1. π^- (1.1 Bev) + xe --> Σ° + K° + residual nucleus
   Σ° --> γ + Λ°
2. γ converts
3. K_1° --> π° + π° (3 of the 4 resulting gammas convert)
4. Λ° --> π° + n
5. and 6. The two gammas from the Λ convert
7. n + xe --> p + residual nucleus

From measurements of the positions of points 1, 4, 5, 6 and 7, and given the masses of the Λ and the neutron, one can compute the mass of the π°. This is possible because the direction of the π° can be determined by the intersection of the plane defined by 4, 5, and 6 with the plane defined by 1, 4, and 7. That is the intersection of the decay plane of the π° with the decay plane of the Λ.

One can show

D1.1 $$M_{\pi^0} = \left[\frac{(B^2 - 4AC)^{1/2} - B}{2A} \right]^{1/2}$$

where

$$A = 4(a^2 + 1)b^2 - e^2$$

$$B = 4(a^2 + 1)M_n^2 - 2C\,e^2$$

$$C = M_\Lambda^2 - M_n^2$$

$$a^2 = \frac{\sin^2(\phi_1 + \phi_2)}{[(\sin\phi_2 + \sin\phi_1)^2 - \sin^2(\phi_1 + \phi_2)]}$$

$$b^2 = \frac{\sin^2\theta_\pi}{\sin^2\theta_n}\, a^2$$

$$e^2 = 2a^2 \frac{\sin\theta_\pi}{\sin\theta_n} \cos(\theta_\pi + \theta_n) - 1$$

and where ϕ_1, ϕ_2, θ_π, and θ_n are defined in Fig. 22.

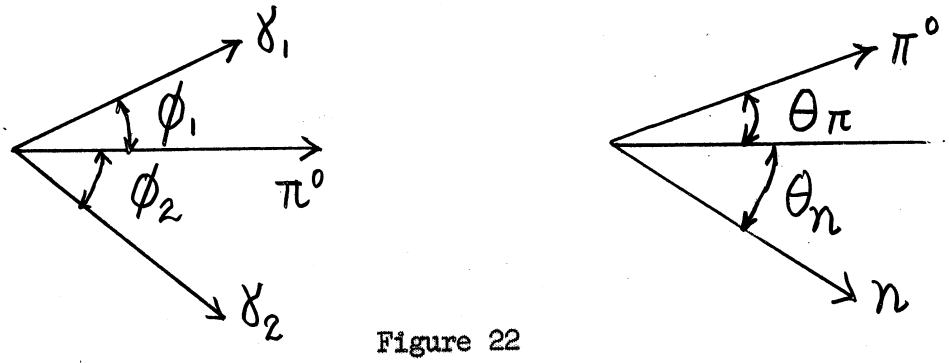

Figure 22

The two stereo views of this event were measured five times, giving π° mass values of 128, 108, 148, 116, and 133 Mev.

The average of these values is 127 ± 6 Mev. Systematic errors were not taken into account.

Appendix E. LISTS OF EVENTS USED IN THE BRANCHING RATIO

ABC events, Part I.

Frame	P_Λ	L_Λ	ω_Λ	$\theta^*_{p,\Lambda}$	$P_{K^\circ_1}$	$L_{K^\circ_1}$	$\omega_{K^\circ_1}$	θ^*_{π,K°_1}
4348	220	3.94	31.1	61	420	3.74	52.3	27
9029	605	10.50	34.4	112	620	4.90	26.5	61
9655	290	6.01	93.1	128	440	1.01	18.0	86
10121	260	scattered		41	320	1.14	147.7	67
10655	1040	4.44	10.4	75	180	0.95	30.4	58
11832	430	3.65	5.9	57	225	1.32	101.4	55
12662	400	4.84	54.4	15	250	0.94	67.9	59
13422	450	4.15	44.2	130	500	1.36	25.1	39
15401	540	8.80	17.1	136	220	3.41	80.2	43
17538	365	6.41	12.7	127	360	1.45	50.8	47
19737	540	0.68	30.9	110	310	1.51	65.9	85
21006	410	1.98	63.1	84	430	0.53	51.1	72
22215	250	0.94	8.7	56	385	0.69	72.4	72
22533	650	0.86	18.4	35	320	6.09	20.9	77
23364	405	3.74	50.4	104	780	0.59	32.1	51
23432	520	2.24	24.1	64	310	0.57	66.8	70
26311	450	0.92	86.6	115	340	3.01	9.4	76
27324	500	1.94	25.8	86	215	0.57	70.2	86
28556	590	2.64	40.3	150	400	0.64	74.6	70
29333	980	3.20	40.4	29	200	0.83	39.6	80
39660	180	0.75	20.9	73	780	2.09	4.5	57
39882	770	3.45	48.5	116	300	0.69	31.7	89
39898	240	1.27	61.0	97	230	0.75	123.7	75
41301	570	3.05	32.8	68	190	1.91	112.4	75
42184	480	2.35	31.7	32	510	1.51	61.2	80
43055	610	1.98	28.4	40	470	4.78	13.2	83
50456	300	2.40	68.3	124	540	1.97	19.6	73
51870	460	2.66	23.7	104	430	3.55	32.1	39
51975	590	2.70	21.1	71	160	1.58	97.3	88
53658	415	scattered		71	260	2.83	22.2	73
55906	355	1.09	18.5	116	460	1.44	63.4	83
57303	610	4.39	31.4	40	580	5.94	15.6	85
59541	840	3.87	18.4	93	410	0.95	50.0	55
59574	250	3.23	61.9	80	280	3.10	46.9	63
60879	870	7.98	10.9	54	410	0.78	33.7	25
61458	590	3.24	28.0	85	580	10.17	24.9	78
62253	230	0.61	92.5	67	340	1.14	30.4	89
64511	510	1.60	19.7	36	580	1.14	12.2	48
66501	520	2.11	12.7	88	650	0.96	18.5	66
67634	600	5.16	48.6	88	200	1.06	78.1	73
68417	540	2.45	77.5	102	650	1.41	47.9	73
71029	490	0.90	65.1	31	460	1.14	82.4	83
71469	275	1.76	43.6	110	260	1.84	91.0	61
74985	550	1.21	14.0	100	580	2.75	14.7	90
75718	640	1.69	7.3	81	270	1.58	27.5	62
77638	1090	3.91	32.5	52	500	1.23	36.3	87
81591	230	1.16	33.3	108	750	3.71	16.3	33

Frame	P_Λ	L_Λ	ω_Λ	$\theta^*_{p,\Lambda}$	P_{K°	L_{K°	ω_{K°	θ^*_{π,K°
82767	700	5.85	9.4	165	190	0.50	89.9	80
83416	460	2.38	9.3	57	380	4.27	127.1	49
84008	340	3.58	148.4	102	500	2.02	22.9	69
84126	480	1.83	40.7	99	460	2.92	27.7	59

ABC events, Part II.

Frame	P_Λ	L_Λ	Λ Potential Path	ω_Λ	$\theta^*_{p,\Lambda}$	$P_{K_1^0}$	$L_{K_1^0}$	K Potential Path	ω_K	$\theta^*_{\pi,K}$
088319	750	1.31	15.21	5.5	98	720	1.62	15.13	2.9	25
088508	740	9.08	11.56	9.8	69	180	2.91	11.72	78.9	76
088509	250	3.90	21.88	12.4	85	300	2.85	23.56	10.6	44
088601	500	2.79	19.07	62.3	87	280	1.32	11.40	70.5	88
089321	250	2.65	16.33	164.2	35	330	0.70	7.74	50.8	22
089794	750	6.34	8.16	23.1	120	240	4.97	5.77	108.4	29
092872	1100	13.37	18.73	11.2	107	270	1.17	21.82	44.0	72
096876	270	2.90	10.53	66.7	108	840	5.30	13.94	8.6	57
097063	390	1.43	12.07	27.2	112	760	3.54	11.37	18.3	77
097840	550	4.41	16.38	60.8	105	360	6.51	11.37	45.9	8
099001	500	11.26	21.34	83.3	83	150	1.59	23.72	124.6	34
099655	800	5.71	20.71	20.1	16	640	0.73	22.25	30.7	65
101202	810	8.42	16.76	40.3	43	270	2.50	14.05	41.5	44
102465	370	4.67	13.92	75.6	76	505	1.44	7.67	35.5	74
103873	660	5.15	26.71	28.2	42	440	3.31	24.05	12.9	82
107774	490	6.15	20.05	47.0	135	520	12.37	18.97	49.2	60
108103	560	4.48	18.56	11.9	56	390	0.70	9.11	86.8	15
108567	190	1.75	9.60	32.8	69	200	1.39	15.76	89.8	80
108839	440	1.25	15.93	8.2	78	530	1.03	16.82	9.7	88
110004	590	1.43	5.00	29.0	136	680	3.16	4.54	24.1	40
110852	890	10.23	16.52	22.2	78	570	1.32	16.84	23.5	81
111916	375	0.71	16.63	67.4	69	410	2.02	16.05	52.4	28
112059	680	2.41	8.72	9.0	87	450	3.60	8.77	27.6	87
112110	250	1.64	12.14	71.1	45	270	3.06	11.39	45.5	31
112647	280	2.23	14.10	50.2	112	470	5.26	11.17	63.0	76
113887	500	1.12	2.13	25.2	95	730	1.39	1.94	14.4	72
114503	660	7.64	15.49	29.3	105	730	5.25	21.26	42.2	66
115971	530	7.53	19.04	41.6	102	460	2.16	15.68	43.8	20
116580	560	0.55	13.82	40.6	116	620	4.55	17.13	38.1	65
116779	280	4.02	4.78	44.3	87	670	2.89	5.69	24.2	75
118712	260	5.69	7.99	43.0	124	530	4.47	9.46	65.9	70
120258	520	1.80	15.60	29.4	46	634	1.08	11.99	26.9	87
121400	420	1.43	8.26	73.9	85	290	3.43	14.83	40.7	36
122063	570	1.47	11.71	33.8	77	720	1.07	15.11	30.2	55
124106	200	1.10	17.13	31.6	45	210	1.74	8.67	107.3	85
128182	880	1.18	10.11	17.1	47	440	3.22	11.43	39.2	65
128540	200	0.79	16.84	37.4	84	810	0.85	13.99	37.3	25
129043	1110	1.50	23.44	7.7	62	210	5.59	16.85	67.4	50
129228	340	3.76	6.35	51.8	67	650	1.31	5.77	37.3	72
129707	650	2.50	11.68	53.2	110	550	2.28	7.40	39.4	80
130724	630	2.20	11.14	29.9	128	465	2.56	15.26	101.4	74
134718	350	2.97	9.96	150.6	145	700	4.06	13.76	26.5	64
136418	620	6.91	13.14	29.4	72	320	4.12	17.35	22.2	69
137873	740	9.29	19.27	11.5	70	280	2.80	6.52	113.3	42
139599	485	4.67	15.65	46.5	73	690	0.86	16.09	14.6	73

ABD events, Parts I and II.

Frame	P_{K°	L_{K°	ω_{K°	$\theta^*_{K^\circ}$	Δ	χ	D_1	D_2	l_1	l_2	L_Λ	ω_Λ
9707	520	2.97	45	47	1.36	86	1.19	3.97	24.4	4.6	4.46	24
19742	430	3.91	63	82	0.50	103	1.78	1.83	16.2	13.2	1.14	126
23397	690	2.21	10	61	0.48	77	2.34	3.99	9.9	14.9	0.81	59
36076	340	3.96	66	47	1.07	128	11.66	1.05	12.4	9.7	2.16	74
40270 Σ°	630	1.41	6	77	0.19	163	0.66	1.25	6.7	13.7	6.80	78
54649	650	1.06	20	80	0.13	76	6.07	8.21	12.7	17.6	6.88	15
59899	310	0.54	50	74	0.02	90	9.95	6.40	11.0	8.5	4.59	49
63285	430	3.47	73	41	0.09	147	1.01	0.19	13.8	7.0	3.70	100
65970	500	1.21	37	46	1.22	86	5.35	5.76	8.1	8.2	3.77	85
67994	210	1.07	33	66	0.60	141	1.77	10.77	6.5	6.0	0.85	41
72242	220	1.25	16	43	0.61	69	3.98	4.78	10.9	8.5	1.87	10
74291	195	0.53	67	40	0.32	106	12.19	0.74	10.9	4.9	1.10	87
* 76644 Σ°	630	0.81	46	34	1.92	130	5.57	13.90	7.8	4.3	3.93	74
77818	170	1.36	155	52	0.33	69	2.60	0.77	18.9	15.5	2.25	72
83858	380	2.14	44	77	0.32	72	0.54	10.82	14.4	16.9	0.61	9
* 87048	440	1.51	50	48	Dalitz pr.		4.74	0	13.4	9.6	5.52	42
88467	300	2.79	74	77	0.01	79	0.55	3.31	8.5	19.6	0.79	49
89784	450	3.65	45	67	1.16	130	9.35	0.07	8.7	13.3	1.40	67
93400	710	3.45	35	27	0.42	109	7.32	4.55	13.8	7.9	1.54	52
94908	240	1.67	97	52	0.31	100	1.21	3.05	5.1	20.1	0.24	62
99237 Σ°	450	5.57	12	59	0.05	90	1.28	7.54	13.7	11.9	1.17	36
101239	390	1.40	13	88	0.43	148	5.12	5.45	11.3	6.0	7.43	30
103521	420	1.56	64	48	0.38	125	3.06	1.63	11.2	19.0	0.99	43
105243	380	2.48	165	28	0.65	130	6.49	0.62	8.6	55.0	2.03	38
* 108197 Σ°	260	2.71	55	65	3 gammas: cannot pair up							
108619	310	4.03	121	48	0.46	80	3.66	2.50	14.7	17.5	1.02	80
111093	390	0.65	69	79	0.02	90	4.59	5.10	11.6	15.3	0.96	27
* 115228	820	1.49	16	86	one gamma ill-defined				14.0	4.8	1.49	40
116671	300	1.10	62	15	1.13	111	0.79	13.49	17.8	21.0	2.40	81
127291	790	3.35	2	66	0.04	94	1.51	3.54	11.3	18.9	0.48	111
128568	500	1.42	70	72	0.14	59	4.73	8.63	26.4	6.4	0.83	70
129418	300	0.96	60	59	0.23	130	2.57	1.72	20.8	10.6	1.98	101
131526	640	0.94	44	88	0.01	69	6.38	5.71	7.2	8.2	3.67	30
135797	330	1.35	18	66	0.23	87	2.85	5.18	17.3	13.3	1.44	102
* 136620 Σ°	730	0.88	86	53	2.19	91	2.41	10.11	7.7	14.7	3.29	78

* = Not used for π° mass determination

Σ° = Three associated gammas, believed to be a case of a neutrally decaying Σ°.

BIBLIOGRAPHY

1. C. Franzinetti and G. Morpurgo, Supplemento al vol. VI, Serie X del Nuovo cimento 2, chapters 4 and 5 (1957).

2. Eisler, Plano, Samios, Schwartz, and Steinberger, Nuovo cimento 5, 1700 (1957).

3. D. Glaser, Proceedings of the Fifth Annual Rochester Conference on High Energy Physics (Interscience Publishers, Inc., New York (1955)).

4. J. L. Brown, D. Glaser, and M. Perl, Phys. Rev. 102, 586 (1956).

5. Brown, Bryant, Burnstein, Glaser, Hartung, Kadyk, Sinclair, Trilling, Vander Velde, and van Putten,

   A. Phys. Rev. Letters 3, 51 (1959)
   B. Phys. Rev. Letters 3, 563 (1959).

6. Mason, Barkas, Dyer, Heckman, Nickols, Smith, Bul. Amer. Phys. Soc. Washington Meeting (1960).

7. Crawford, Cresti, Good, Stevenson, and Ticho, Phys. Rev. Letters 2, 114 (1959).

8. High Energy Conference, Kiev (1959)

9. Nordin, Orear, Reed, Rosenfeld, Solmitz, Taft, and Tripp, Phys. Rev. Letters 1, 380 (1958).

10. Crawford, Cresti, Douglass, Good, Kalbfleisch, Stevenson, and Ticho, Phys. Rev. Letters 2, 226 (1959).

11. Crawford, Cresti, Good, Gottstein, Lyman, Solmitz, Stevenson, and Ticho, 1958 Annual Conference on High Energy Physics at CERN, appendix I.

12. Cronin, Cork, Kerth, Wenzel, and Cool, Bul. Amer. Phys. Soc. New York Meeting (1960).

13. "Asymmetry in the Decay of the Σ Hyperon", Cool, Cork, Cronin, and Wenzel, Phys. Rev. 114, 912 (1959).

14. A π° of isotopic spin zero has been proposed, but even if this particle were to occur in the Λ decay rather than the ordinary isotopic spin 1 meson, there should be no detectable difference as the lifetimes for the two neutral particles for 2-gamma decay would be expected to be about the same. c.f. A. M. Baldin, Nuovo cimento VIII, 569 (1958).

15. Davisson and Evans, Reviews of Modern Physics, 24, 79 (1952), equations 60 and 61. Davies, Bethe, and Maximon, Phys. Rev. 93, 788 (1954).

16. R. R. Wilson, Phys. Rev. 84, 100 (1951).

17. M. S. Bartlett, Phil. Mag. 44, 249 (1953).

18. E. Fermi, Nuovo cimento 2, Supplemento 1, 54 (1955).

19. H. L. Anderson, Sixth Rochester Conference (1956).

20. M. Gell-Mann and A. Pais, Proc. of International Conference on High Energy Physics (Pergamon, London (1955)).

21. Okubo, Marshak, and Sudarshan, Phys. Rev. 113, 944 (1959).